Calreticulin, a Molecular Chaperone in the Endoplasmic Reticulum, Modulates Radiosensitivity of Human Glioblastoma U251MG Cells

Tomohiro Okunaga,[1,2] Yoshishige Urata,[1] Shinji Goto,[1] Takayuki Matsuo,[2] Shingo Mizota,[1,2] Keisuke Tsutsumi,[2] Izumi Nagata,[2] Takahito Kondo,[1] and Yoshito Ihara[1,3]

[1]Department of Biochemistry and Molecular Biology in Disease, Atomic Bomb Disease Institute; [2]Department of Neurosurgery, Nagasaki University Graduate School of Biomedical Sciences, Nagasaki, Japan; and [3]Core Research for Evolutional Science and Technology, Japan Science and Technology Agency, Kawaguchi, Japan

Abstract

Radiotherapy is the primary and most important adjuvant therapy for malignant gliomas. Although the mechanism of radiation resistance in gliomas has been studied for decades, it is still not clear how the resistance is related with functions of molecular chaperones in the endoplasmic reticulum. Calreticulin (CRT) is a Ca^{2+}-binding molecular chaperone in the endoplasmic reticulum. Recently, it was reported that changes in intracellular Ca^{2+} homeostasis play a role in the modulation of apoptosis. In the present study, we found that the level of CRT was higher in neuroglioma H4 cells than in glioblastoma cells (U251MG and T98G), and was well correlated with the sensitivity to γ-irradiation. To examine the role of CRT in the radiosensitivity of malignant gliomas, the *CRT* gene was introduced into U251MG cells, which express low levels of CRT, and the effect of overexpression of CRT on the radiosensitivity was examined. The cells transfected with the *CRT* gene exhibited enhanced radiation-induced apoptosis compared with untransfected control cells. In CRT-overexpressing cells, cell survival signaling via Akt was markedly suppressed. Furthermore, the gene expression of protein phosphatase 2Acα (PP2Acα), which is responsible for the dephosphorylation and inactivation of Akt, was up-regulated in CRT-overexpressing cells, and the regulation was dependent on Ca^{2+}. Thus, overexpression of CRT modulates radiation-induced apoptosis by suppressing Akt signaling through the up-regulation of PP2Acα expression via altered Ca^{2+} homeostasis. These results show the novel mechanism by which CRT is involved in the regulation of radiosensitivity and radiation-induced apoptosis in malignant glioma cells. (Cancer Res 2006; 66(17): 8662-71)

Introduction

The management of patients with glioblastoma multiforme is difficult and poor results have led to a search for novel therapeutic approaches (1). Radiotherapy is the most effective adjuvant modality in the management of glioblastoma multiforme, doubling the median survival rate (2). Radiation-induced cell death is associated with a complex interaction of various factors. The cellular targets of radiation-induced apoptosis are the plasma membrane, cytosol, and nuclear DNA (3). The mechanisms of radiation-induced apoptosis have been studied extensively in terms of p53 status, the Bcl-2 gene family, the Fas-mediated pathway, the ceramide-mediated pathway, the caspase cascade, and the ataxia-telangiectasia-mutated gene (3–5). Nevertheless, it still remains unclear which macroscopic or molecular features determine the response of glioblastoma multiforme to irradiation. For instance, although most studies have shown an association between p53 status and the response to radiotherapy (6), no such association has been convincingly shown in glioblastoma multiforme patients (7).

Recently, it was reported that the Ca^{2+} of the endoplasmic reticulum and/or cytoplasm plays an important role in radiation-induced apoptosis in association with some of these mechanisms (8–12). In the p53 pathways, Ca^{2+} and S100B regulated p53-dependent cell growth arrest and apoptosis (8). Bcl-2 and related proteins interfere with intracellular stores and the release of Ca^{2+} (13). Moreover, ceramide induces an increase in the cytoplasmic Ca^{2+} concentration by releasing Ca^{2+} from intracellular stores and activating the capacitative Ca^{2+} entry pathway, and deletion of Ca^{2+} from stores is a key to the protective action of Bcl-2 against apoptosis (11). In ataxia-telangiectasia cells, the mobilization of Ca^{2+} either was absent or increased slowly postirradiation (14). These findings indicate that changes in intracellular Ca^{2+} homeostasis play a role in the modulation of apoptosis (15).

Calreticulin (CRT) was initially found as a Ca^{2+}-binding protein in the lumen of the endoplasmic reticulum (16). CRT is a multifunctional protein involved in many biological processes that include the regulation of Ca^{2+} homeostasis (16), intercellular or intracellular signaling, gene expression (17), glycoprotein folding (18), and nuclear transport (19). We found that overexpression of CRT enhanced apoptosis in myocardiac H9c2 cells under conditions inductive to differentiation with retinoic acid (20) or under oxidative stress (21). Moreover, CRT regulates p53 function to induce apoptosis by affecting the rate of degradation and nuclear localization of p53 (12). Furthermore, there have been few reports related to the molecular chaperones and radiation-induced apoptosis of glioma (22). However, it is still not clear whether CRT is involved in the regulatory mechanism for the radiation-induced apoptosis.

In the present study, we investigated the role of CRT in radiosensitivity and radiation-induced apoptosis, using human glioma cell lines. We show here that overexpression of CRT modulates the radiosensitivity of human glioblastoma cells by suppressing Akt/protein kinase B signaling for cell survival via alterations of cellular Ca^{2+} homeostasis.

Requests for reprints: Yoshito Ihara, Department of Biochemistry and Molecular Biology in Disease, Atomic Bomb Disease Institute, Nagasaki University Graduate School of Biomedical Sciences, 1-12-4 Sakamoto, 852-8523 Nagasaki, Japan. Phone: 81-95-849-7099; Fax: 81-95-849-7100; E-mail: y-ihara@net.nagasaki-u.ac.jp.

doi:10.1158/0008-5472.CAN-05-4256

Materials and Methods

Antibodies and reagents. Antibodies against CRT, calnexin, Grp94, and Erp57 were purchased from Stressgen Biotech Corp. (Victoria, British Columbia, Canada). The anti-Akt and antiphosphorylated Akt (Ser^{473}, Thr^{309}) antibodies were purchased from Cell Signaling Technology (Beverly, MA). The anti–protein phosphatase 2A catalytic subunit α (PP2Acα) antibody was from BD Transduction Laboratories (Lexington, KY). The antibodies against PP2A regulatory protein 65 (PP2A-RP65) and PP1a were from Santa Cruz Biotechnology (Santa Cruz, CA). The anti-glyceraldehyde 3-phosphate dehydrogenase (GAPDH) antibody was purchased from Chemicon International (Temecula, CA). The reagents used in the study were all of high grade from Sigma or Wako Pure Chemicals (Osaka, Japan).

Cell culture. Two human glioblastoma cell lines (U251MG and T98G) and a human neuroglioma cell line (H4) were used in this study. The U251MG cells were obtained from Human Science Research Resource Bank (Osaka, Japan). The T98G and H4 cells were obtained from American Type Culture Collection (Manassas, VA). These cells and the *CRT* gene–transfected U251MG cells were cultured in DMEM supplemented with 10% FCS in a humidified atmosphere of 95% air and 5% CO_2 at 37°C. The culture medium was replaced every 2 days.

Gene transfection and selection of cells. A full-length mouse CRT cDNA was cloned from total RNA of mouse RAW264.7 cells by reverse transcription-PCR, and cloned into the mammalian expression plasmid pcDNA3.1 (Invitrogen, Tokyo, Japan) as described before (20). Myr-Akt1 in pUSEamp(+), an expression vector for myristoylated Akt, was obtained from Upstate (Lake Placid, NY). The gene expression vectors were introduced into U251MG cells using LipofectAMINE Plus reagent (Invitrogen) according to the directions from the manufacturer. Stable transfectants were screened by culturing with 500 μg/mL G418. The cloned G418-resistant lines were then screened for expression of CRT. Two independent clonal cell lines (CRT-M5 and CRT-M6) found to express high levels of CRT upon immunoblot analysis were selected and used for the experiments.

Terminal deoxynucleotidyltransferase-mediated dUTP nick end labeling assay. Apoptosis was detected by flow cytometry with the terminal deoxynucleotidyltransferase-mediated dUTP nick end labeling (TUNEL) method (23) using an Apop Tag Plus fluorescein *in situ* apoptosis detection kit (Chemicon International).

Immunoblot analysis. Cultured cells were harvested and lysed in lysis buffer [20 mmol/L Tris-HCl (pH 7.5), 130 mmol/L NaCl, and 1% NP40 including protease inhibitors (20 μmol/L amidinophenyl methanesulfonyl fluoride, 50 μmol/L pepstatin, and 50 μmol/L leupeptin)]. Protein samples were subjected to SDS-PAGE and then transferred to a nitrocellulose membrane as described (21). The membrane was blocked and then incubated with the primary antibody in TBS containing 0.05% Tween 20. The blots were coupled with the peroxidase-conjugated secondary antibodies, washed, and then developed using the ECL chemiluminescence detection kit (GE Healthcare Bioscience, Tokyo, Japan) according to the instructions from the manufacturer.

Cell survival assay and analysis. The cells were trypsinized in a 0.05% trypsin/1 mmol/L EDTA solution and replated in specified numbers into 60-mm dishes for determination of colony-forming ability (24). One day after, these dishes were irradiated with a dose of 0 to 10 Gy. A ^{60}Co source was used for the γ-irradiation of cells. After 14 days of incubation, the contents of the dishes were stained with a Giemsa stain solution (Muto Pure Chemicals, Tokyo, Japan), colonies with >50 cells were counted, and the radiation-surviving fraction (plating efficiency of experimental group/plating efficiency of control group) was determined. Survival curves were generated by combining data from four independent experiments in accordance with linear-quadratic fitting (KaleidaGraph software 4.0).

Protein phosphatase assay. Protein Ser/Thr phosphatase activity was assayed photometrically using Ser/Thr Phosphatase Assay Kit 1 (Upstate), according to the directions from the manufacturer. The activity was assayed in the presence or absence of 10 nmol/L okadaic acid, and the okadaic acid–sensitive activity was estimated as PP2A-specific activity. The phosphopeptide (R-K-pT-I-R-R) was used as a phosphatase substrate. Protein concentrations were determined using a BCA assay kit (Pierce, Rockford, IL).

Northern blot analysis. The full-length rat PP1a catalytic subunit and PP2A catalytic α cDNAs were generously provided by Dr. Kunimi Kikuchi (Hokkaido University, Hokkaido, Japan; refs. 25, 26). A *Pst*I-*Sma*I fragment of 600 bp and *Eco*RI-*Pvu*II fragment of 680 bp were prepared from the cDNAs of PP1ac and PP2Acα, respectively, and used as cDNA probes. The probes were labeled with ^{32}P using a Random Primer Labeling kit (Takara Biomedicals, Shiga, Japan). The isolation of cytoplasmic RNA and Northern blotting were essentially done as described before (27).

Assays for release and uptake of Ca^{2+} in the cell. For the $^{45}Ca^{2+}$ release assay, cells were cultured for 48 hours with medium containing $^{45}Ca^{2+}$ (1 μCi/mL). After washing with Ca^{2+}-free Earle's balanced salt solution (EBSS; Invitrogen) containing 3 mmol/L EGTA, cells were detached from the culture plates with trypsinization buffer (0.25% trypsin and 0.02% EDTA in EBSS), and the cell suspensions were preincubated in Ca^{2+}-free EBSS at 37°C for 3 minutes and sequentially stimulated with thapsigargin (0.1 μmol/L), ionomycin (2 μmol/L), and monensin (2 μmol/L). The cell suspensions were collected 5 minutes after the addition of each reagent and centrifuged. The radioactivity released from the cells was measured in the supernatant. Cell pellets were lysed and protein amounts were determined using a BCA assay kit (Pierce). $^{45}Ca^{2+}$ release was expressed as the cpm subtracted from those recovered in the preceding collection, and normalized to the protein in the corresponding cell pellets. The uptake of Ca^{2+} was measured radiometrically using the Millipore filtration technique as described previously (21) with a slight modification. The cells were irradiated (5 Gy) for the periods indicated, then washed with EBSS and cultured for 10 minutes in EBSS containing $^{45}Ca^{2+}$ (5 μCi/mL). Cells were detached from the culture plates by trypsinization buffer, and the cell suspension was filtered through a 0.45-μm nitrocellulose filter (Bio-Rad, Tokyo, Japan) under vacuum conditions. The filters were rinsed twice with 0.5 mL washing buffer [10 mmol/L HEPES (pH 7.4), 150 mmol/L KCl, 2 mmol/L EGTA, and 2.5 mmol/L $MgCl_2$]. $^{45}Ca^{2+}$ uptake was calculated by measuring the radioactivity and standardized using protein concentrations.

Measurement of intracellular free calcium. The cytoplasmic free Ca^{2+} concentration, $[Ca^{2+}]_i$, was measured with a dual-excitation wavelength spectrofluorophotometer (RF-5500, Shimadzu, Kyoto, Japan) using the fluorescent Ca^{2+} indicator Fura-2 tetra (acetoxymethyl) ester (Fura-2-AM) essentially as described previously (21).

Luciferase activity assay. Luciferase reporter constructs for the rat PP2Acα gene promoter [i.e., pGL3-pro-PP2Ac, pGL3-pro-PP2Ac (C3), and pGL3-pro-PP2Ac (C3-Mut/C)] were prepared using the reporter vector pGL3-Basic (Stratagene, Tokyo, Japan) as described previously (27). Each vector was transfected into cells by using LipofectAMINE 2000 (Invitrogen) according to the instructions from the manufacturer. After 24 hours of transfection, cells were treated with thapsigargin (5 μmol/L) or BAPTA-AM (10 μmol/L) or left untreated for the periods indicated in the text. Then, luciferase activity was assayed with cellular extracts by using a Dual-Luciferase Reporter Assay System (Promega, Tokyo, Japan).

Statistical analysis. Statistical analysis was done using Student's *t* test or ANOVA (StatView software). Significance was set at $P < 0.05$.

Results

Radiosensitivity and expression levels of CRT in human glioma cell lines. To investigate whether the expression level of endoplasmic reticulum chaperones differs in accordance with the radiosensitivity of glia-derived malignant cells, human neuroglioma (H4) and glioblastoma (U251MG and T98G) cells were selected as different categories of glioma. First, to examine the radiosensitivity of each cell line, the colony-forming ability of the cells after γ-irradiation (0-10 Gy) was evaluated, as described in Materials and Methods. As shown in Fig. 1A, H4 exhibited a significant decrease in the surviving fraction after γ-irradiation, compared with U251MG and T98G cells. These results indicate that H4 cells are highly susceptible to irradiation compared with U251MG and T98G cells, suggesting that radiosensitivity differs in different categories of glioma. In Fig. 1B, the expression of endoplasmic reticulum

resident chaperones or proteins, such as CRT, calnexin, Grp94, and Erp57, was examined by immunoblot analysis using specific antibodies, and compared between the cell lysate samples. The level of CRT was apparently higher in H4 cells than U251MG or T98G cells. On the other hand, the expression levels of calnexin, Grp94, and Erp57 did not show a significant difference among the cell types.

Establishment of *CRT* gene–overexpressing U251MG cells. To investigate the biological significance of the level of CRT to the radiosensitivity of glioma cells, a *CRT* gene expression vector was constructed and introduced into U251MG cells as described in Materials and Methods. U251MG cells were chosen because they expressed a relatively low level of CRT compared with H4 cells (Fig. 1B). After screening by culturing with G418, the expression level of CRT was characterized immunologically in the G418-resistant transfectants. Two transfectants (CRT-M5 and CRT-M6) expressing high levels of CRT were established and used in subsequent experiments. Figure 2*A* shows that the expression of CRT increased in CRT-M5 and CRT-M6 cells compared with the parental and mock-transfected (Vector8) U251MG cells. The transfection had no apparent effect on the expression of other endoplasmic reticulum chaperones, such as calnexin and Grp94 (data not shown). Next, the intracellular distribution of CRT was examined by indirect immunofluorescence microscopy, as shown in Fig. 2*B*. The immunoreactivity for CRT distributed in a perinuclear granular pattern in all cases, including the control and gene-transfected cells, although the signal intensity was increased in the transfectants compared with the control cells (*arrows*).

Effect of overexpression of CRT on radiosensitivity of U251MG cells. To evaluate the effect of overexpressed CRT on radiosensitivity in U251MG cells, colony-forming ability was examined after 14 days of γ-irradiation in control (Vector8) and CRT-overexpressing (CRT-M5 and CRT-M6) cells (Fig. 2*C*). The colony-forming ability markedly decreased in CRT-overexpressing cells compared with control cells. These results indicate that overexpression of CRT enhances the radiation-induced cell damage in U251MG cells. To further characterize the enhanced radiation-induced cell damage in CRT-overexpressing cells, apoptotic characteristics were examined by TUNEL assay as described in Materials and Methods (Fig. 2*D*). Among control cells (Vector8), TUNEL-positive cells bearing DNA-strand breaks appeared after 72 hours of γ-irradiation, and then decreased after 96 hours. In contrast, among CRT-overexpressing cells (CRT-M5), the TUNEL-positive cells appeared after 72 hours of γ-irradiation, and were still detectable 96 hours later. In the assay, some damaged cells were detached from culture plates and removed during the washing step, and the remaining cells attached to the plates were examined, especially after 96-hour exposure to irradiation. As a result, the population of less-damaged surviving clonogens (TUNEL-negative) might be increased in controls than in CRT-overexpressing cells after 96 hours. These results suggest that overexpression of CRT enhances radiation-induced apoptosis, resulting in the enhanced suppression of the ability of U251MG cells to form colonies after γ-irradiation.

Overexpression of CRT suppresses Akt/protein kinase B activity after γ-irradiation. The Akt pathway is known as a pivotal cell survival signal in the cell (28). We previously reported that overexpression of CRT suppressed Akt activity during the cardiac differentiation of H9c2 cells (20). Therefore, we also focused on the Akt pathway in CRT-overexpressing cells treated with irradiation. In Fig. 3*A*, the phosphorylation status of Akt was examined in control and CRT-overexpressing cells treated with γ-irradiation by immunoblot analysis using the antibodies against phosphorylated Akt. In control cells, the levels of Akt phosphorylated at both Ser^{473} and Thr^{309} were increased at 3 hours after the irradiation. On the other hand, in CRT-overexpressing cells, levels of phosphorylated Akt were unchanged after the irradiation. To confirm the functional link between phosphorylation status and activity in Akt, the cells were treated with or without γ-irradiation (5 Gy), and Akt activity was examined after 3 hours, by assessing the phosphorylation of GSK-3α/β, a substrate of Akt kinase, as described in Materials and Methods (Fig. 3*B*). Akt was not activated by γ-irradiation in CRT-overexpressing cells, in spite of the marked activation of Akt in control cells treated with γ-irradiation. These results are consistent with the results for the phosphorylation status of Akt in control and CRT-overexpressing cells treated with γ-irradiation.

Constitutive activation of Akt protects against radiation-induced apoptosis in U251MG cells. To investigate whether the activation of Akt contributes to cellular protection against irradiation in U251MG cells, an expression vector for myristoylated

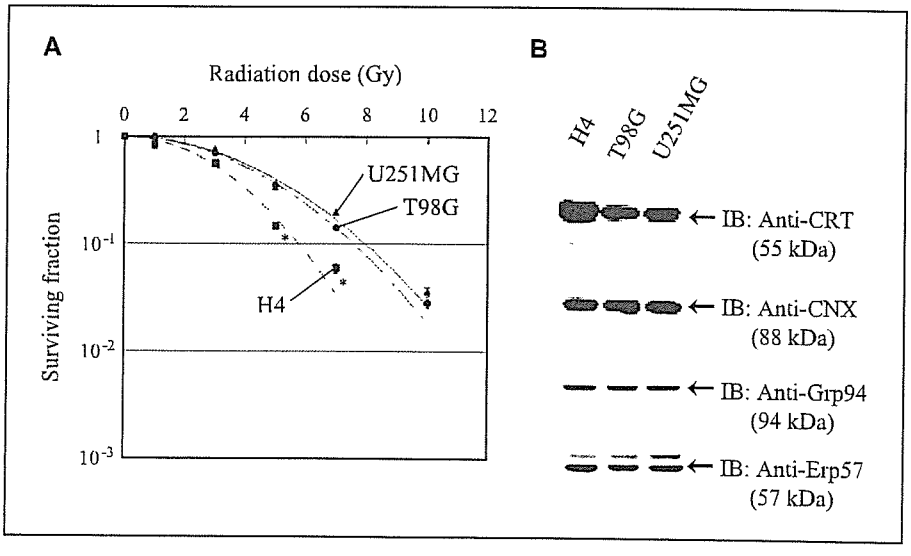

Figure 1. The expression of CRT is up-regulated in radiosensitive neuroglioma H4 cells. *A*, radiosensitivity was evaluated in human neuroglioma (H4) and glioblastoma (T98G and U251MG) cells by colony-forming assay after γ-irradiation (5 Gy) as described in Materials and Methods. ■, H4; ●, T98G; ▲, U251MG. *Points*, mean of four experiments; *bars*, SD. *, $P < 0.01$ versus same dose of irradiation for U251MG and T98G. *B*, expression levels of endoplasmic reticulum chaperones [i.e., CRT, calnexin (*CNX*), Grp94, and Erp57] were examined in H4, T98G, and U251MG cells by immunoblot analysis using specific antibodies as described in Materials and Methods.

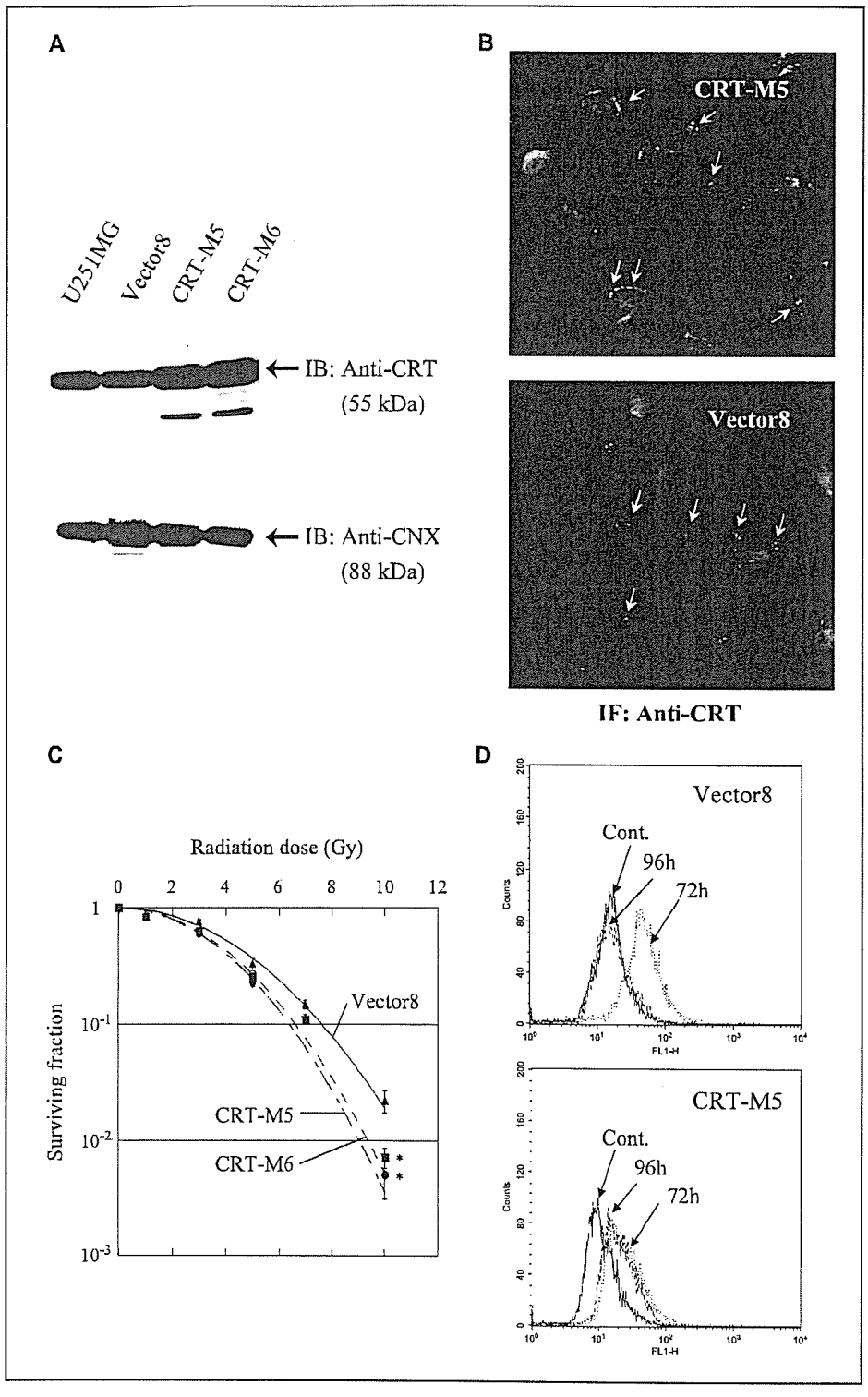

Figure 2. Overexpression of CRT enhances radiation-induced cell death in U251MG cells. *A*, U251MG cells were transfected with the expression vector for the *CRT* gene, and antibiotic-resistant cell lines were established as described in Materials and Methods. The expression level of CRT was examined by immunoblot analysis in parental cells and cells transfected with a mock vector (Vector8) and the CRT gene expression vector (CRT-M5 and CRT-M6). *B*, the intracellular distribution of CRT was examined by indirect immunofluorescence (*IF*) microscopy using a specific antibody in control and gene-transfected cells. *C*, radiosensitivity was evaluated based on colony-forming ability after γ-irradiation (5 Gy) as described in Materials and Methods in control and *CRT* gene–transfected cells. ▲, Vector8; ●, CRT-M5; ■, CRT-M6. *Points*, mean of at least four experiments; *bars*, SD. *, $P < 0.01$ versus same dose of irradiation (10 Gy) for Vector8. *D*, control (Vector8) and gene-transfected (CRT-M5) cells were irradiated (5 Gy) for 10 minutes. Then, at 72 and 96 hours postirradiation, DNA double-strand breaks were detected by the TUNEL method as described in Materials and Methods.

Akt (Myr-Akt1) was introduced into the CRT-overexpressing cells as described in Materials and Methods, to generate cells in which Akt is constitutively activated. After 24 hours of transfection, the expression of Myr-Akt1 was detected by immunoblot analysis using the anti-myc antibody (Fig. 3*C*). Then, the cells were treated with γ-irradiation (5 Gy), and apoptosis was estimated after 72 hours, by the TUNEL assay as described above. As shown in Fig. 3*D*, although TUNEL-positive cells were detected among CRT-overexpressing cells, numbers were diminished in the cells transfected with the Myr-Akt expression vector, indicating that activation of Akt plays an important role in cytoprotection against irradiation. This also suggests that a suppressed Akt pathway is a cause of the enhanced susceptibility to radiation-induced apoptosis in CRT-overexpressing cells.

PP2A is up-regulated in CRT-overexpressing U251MG cells. Ionizing radiation is known to trigger the Akt pathway through the activation of epidermal growth factor receptor families and phosphatidylinositol 3-kinase (PI3K; refs. 29, 30). To establish whether overexpression of CRT affects the activity of PI3K, a signaling molecule upstream of Akt, we examined PI3K activity in control and CRT-overexpressing cells treated with γ-irradiation (5 Gy). However, PI3K activity was not suppressed in CRT-overexpressing cells after the irradiation, but rather was slightly increased, compared with that in control cells (data not shown). This suggests that the suppression of the radiation-induced activation of Akt in CRT-overexpressing cells is due to enhanced inactivation of Akt by PP2A (20, 31). In fact, the phosphorylation of Akt was apparently up-regulated in CRT-overexpressing cells treated with okadaic acid (100 nmol/L), a specific inhibitor of PP2A (data not shown). To investigate whether PP2A is influenced by overexpression of CRT, PP2A activity was assayed with cell lysates from control and CRT-overexpressing cells treated with or without γ-irradiation (5 Gy). In Fig. 4*A*, PP2A activity was always greater in CRT-overexpressing cells rather than controls, although the activity was slightly suppressed by irradiation in both cells. Next, the expression of phosphatases was examined at the level of

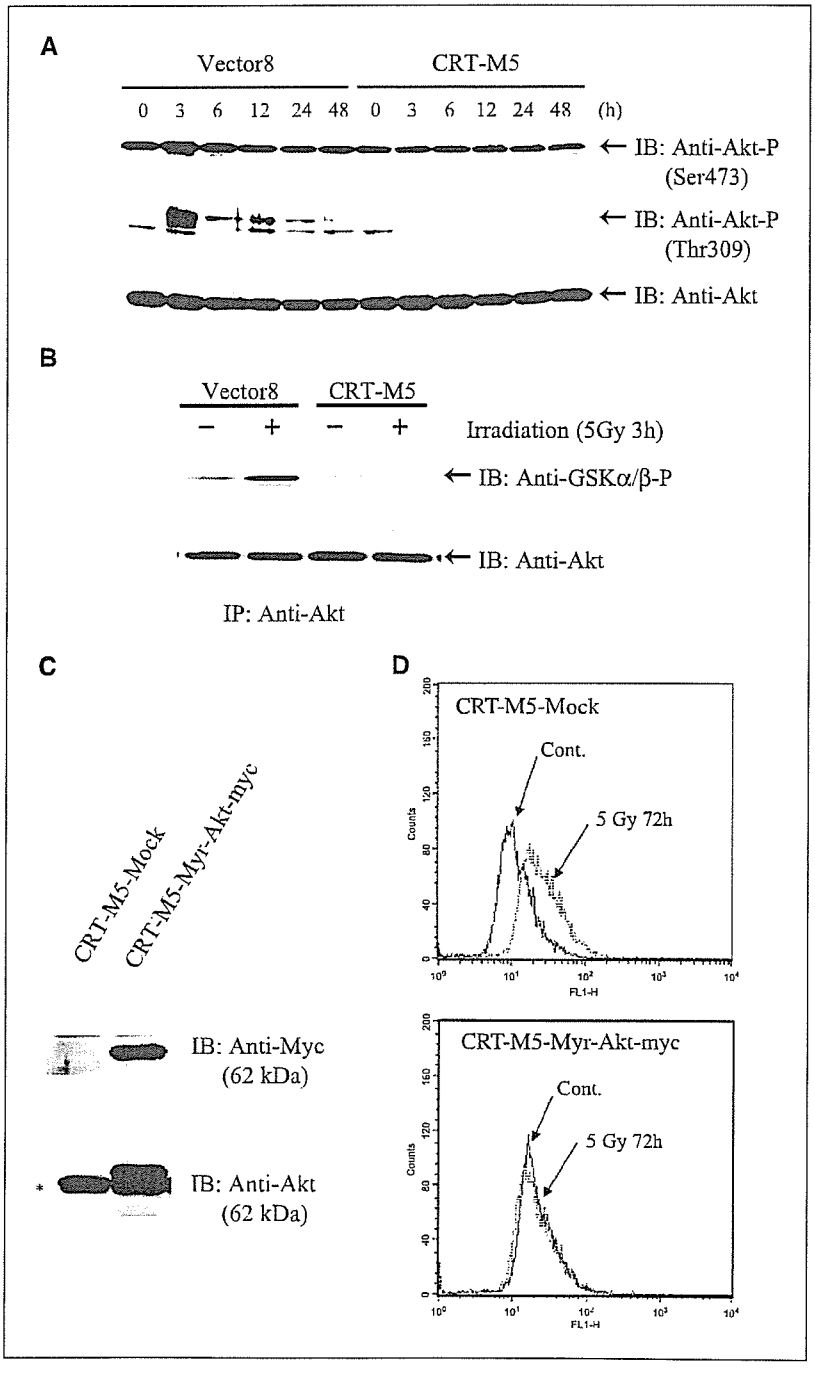

Figure 3. Radiation-induced activation of Akt is suppressed in CRT-overexpressing cells. *A*, the phosphorylation status of Akt was examined in control (Vector8) and CRT-overexpressing (CRT-M5) cells treated with γ-irradiation (5 Gy) by immunoblot analysis using antibodies against Akt phosphorylated at Ser^{473} and Thr^{309} as described in Materials and Methods. *B*, Akt activity was examined in control and CRT-overexpressing cells at 3 hours after the treatment with or without γ-irradiation (5 Gy) by estimating the phosphorylation of GSK-3α/β as described in Materials and Methods. *C*, CRT-overexpressing cells (CRT-M5) were transiently transfected with a mock vector or the expression vector for the myristoylated Akt gene (*Myr-Akt1*) to overexpress active Akt as described in Materials and Methods. The expression of myristoylated Akt was examined by immunoblot (*IB*) analysis using the anti-myc antibody in cells transfected with the mock vector (CRT-M5-Mock) and Myr-Akt1 (CRT-M5-Myr-Akt-myc). *, endogenous Akt. *D*, after 24 hours of transfection with the mock or Myr-Akt1, the cells were irradiated (5 Gy); then, at 72 hours postirradiation, cell damage was estimated by the TUNEL method as described above.

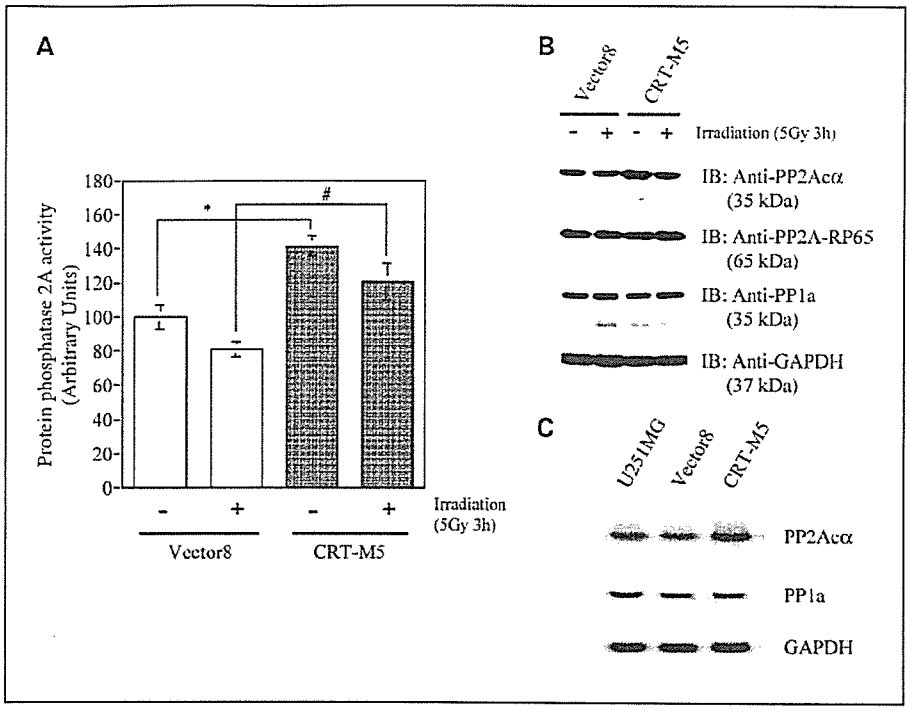

Figure 4. The expression of PP2A is up-regulated in CRT-overexpressing cells. *A*, the activity of PP2A was assayed in control (Vector8) and CRT-overexpressing (CRT-M5) cells at 3 hours after the treatment with or without γ-irradiation (5 Gy). *Columns*, mean of at least three experiments; *bars*, SD. *, $P < 0.05$ versus untreated Vector8 cells. #, $P < 0.05$ versus Vector8 cells treated with irradiation. *B*, the protein levels of protein Ser/Thr phosphatases (i.e., PP2Acα, PP2A-RP65, and PP1a) and GAPDH were examined by immunoblot analysis using specific antibodies in control and CRT-overexpressing cells at 3 hours after the treatment with or without γ-irradiation (5 Gy). *C*, transcriptional expression of PP2Acα, PP1a, and GAPDH was examined in control and CRT-overexpressing cells by Northern blot analysis as described in Materials and Methods.

the protein of transcription by conducting immunoblot and Northern blot analyses, respectively. In Fig. 4*B*, the protein level of PP2Acα increased in CRT-overexpressing cells, compared with controls. However, no significant change was observed in the levels of PP2A regulatory protein 65 (PP2A-RP65), PP1a, and GAPDH between control and CRT-overexpressing cells. Furthermore, the expression of PP2Acα was up-regulated at the transcriptional level in CRT-overexpressing cells (Fig. 4*C*). Together, these results indicate that PP2Acα is transcriptionally up-regulated in CRT-overexpressing cells. They also support that PP2A activity is increased by the up-regulated expression of PP2Acα in the CRT-overexpressing cells.

Ca^{2+} homeostasis and responses to irradiation are altered in CRT-overexpressing U251MG cells. We previously reported that the gene expression of PP2Ac was controlled by altered Ca^{2+} homeostasis in myocardiac H9c2 cells (27). To investigate the effect of CRT overexpression on cellular Ca^{2+} homeostasis, intracellular Ca^{2+} pools were characterized in control and CRT-overexpressing cells. After 48 hours of loading with $^{45}Ca^{2+}$, the cells were washed and resuspended in Ca^{2+}-free buffer. Unidirectional fluxes to the extracellular medium after stimulation with several Ca^{2+} modulators were then measured as described in Materials and Methods. Thapsigargin, an inhibitor of sarcoplasmic/endoplasmic reticulum Ca^{2+}-ATPase (SERCA), ionomycin, a Ca^{2+} ionophore, and monensin, another ionophore affecting acidic stores, were used to stimulate the cellular Ca^{2+} pools (Fig. 5*A*). The results showed that cellular Ca^{2+} contents were apparently increased mainly in the thapsigargin-sensitive Ca^{2+} pools of CRT-overexpressing cells, compared with controls, suggesting that Ca^{2+} stores in the endoplasmic reticulum were increased in CRT-overexpressing cells. We next examined $[Ca^{2+}]_i$ in control and CRT-overexpressing cells after treatment with irradiation (5 Gy). As shown in Fig. 5*B*, $[Ca^{2+}]_i$ was markedly higher in CRT-overexpressing cells than controls at 30 minutes after γ-irradiation (5 Gy), although it increased by γ-irradiation in both cells.

In U937 cells lacking inositol 1,4,5-triphosphate receptor (IP3R) 1, the irradiation-induced increase of $[Ca^{2+}]_i$ is significantly suppressed, suggesting that Ca^{2+} stores in the endoplasmic reticulum plays an important role in the irradiation-induced increase of $[Ca^{2+}]_i$ (32). To investigate whether the IP3R-dependent release of Ca^{2+} from the endoplasmic reticulum is involved in the mechanism, the effect of xestospongin C (5 μmol/L), an inhibitor of IP3R (21) on the irradiation-induced increase of $[Ca^{2+}]_i$ in control and CRT-overexpressing cells was examined. As shown in Fig. 5*C*, with xestospongin C, the irradiation-induced increase of $[Ca^{2+}]_i$ was apparently suppressed in both control and CRT-overexpressing cells; however, the levels were still higher than those of nontreated cells. On the other hand, when the cells were pretreated with Ni^{2+} (5 mmol/L) to block Ca^{2+} influx from the extracellular space through Ca^{2+} channels and Na^+/Ca^{2+} exchangers in the plasma membrane (33), the irradiation-induced increase of $[Ca^{2+}]_i$ was significantly suppressed to reach the levels of nontreated cells. To further investigate the effect of CRT overexpression on irradiation-induced Ca^{2+} influx from the extracellular spaces, $^{45}Ca^{2+}$ uptake was examined in control and CRT-overexpressing cells after treatment with irradiation as described in Materials and Methods. As shown in Fig. 5*D*, the uptake of $^{45}Ca^{2+}$ was apparently enhanced in CRT-overexpressing cells after 30-minute exposure to irradiation, compared with controls, although the uptake increased in both control and CRT-overexpressing cells. Together, these results indicate that the IP3R-sensitive release of Ca^{2+} and Ca^{2+} influx from the extracellular space both play important roles in the mechanism of the irradiation-induced increase of $[Ca^{2+}]_i$ in the cells, and were enhanced by the overexpression of CRT.

The gene promoter activity of PP2Acα is up-regulated in CRT-overexpressing cells through cytoplasmic free Ca^{2+}. In the PP2Acα gene promoter, cyclic AMP response element (CRE) is a pivotal transcription site, through which the activation is regulated by $[Ca^{2+}]_i$, although both the GC-box and CRE additively contribute

to the basal promoter activity (27). To investigate whether the CRE-dependent gene expression of PP2Acα is influenced by the overexpression of CRT, the gene promoter activity was examined by assaying the luciferase activity as described in Materials and Methods. Control and CRT-overexpressing cells were transfected with various luciferase vectors [i.e., pGL3-pro-PP2Ac, which contains the entire promoter sequence of PP2Aca (−1,209 to +258); pGL3-pro-PP2Ac (C3), which contains a CRE but no GC-box (−145 to +258); and pGL3-pro-PP2Ac (C3-Mut/C) in which the CRE is disabled by mutation (−145 to +258)]. After 24 hours of transfection, cell lysates were prepared and subjected to an assay for luciferase activity. As shown in Fig. 6*A*, the level of activity was higher in CRT-overexpressing cells than controls when either pGL3-pro-PP2Ac or pGL3-pro-PP2Ac (C3) was transfected. However, in the case of pGL3-pro-PP2Ac (C3-Mut/C), no activity was detected in the control or CRT-overexpressing cells. These results indicate that the activity of the PP2Acα promoter is up-regulated by overexpression of CRT through the CRE. Next, to investigate whether the enhancing effect of overexpressed CRT on the PP2Acα promoter is regulated through the change in $[Ca^{2+}]_i$, we examined the promoter activity in control and CRT-overexpressing cells treated with Ca^{2+} modulators such as thapsigargin and BAPTA-AM. Thapsigargin and BAPTA-AM, a cell-permeable Ca^{2+} chelator, were used to increase and decrease $[Ca^{2+}]_i$ in the cell, respectively (27). In Fig. 6*B*, control cells transfected with pGL3-pro-PP2Ac (C3) were treated with or without thapsigargin (5 μmol/L for 2 hours), and then the luciferase activity was assayed as described above. The results showed that the activity of the PP2Acα promoter was up-regulated in control cells by the increase of $[Ca^{2+}]_i$ with thapsigargin treatment. These findings are consistent with those in the case of myocardiac H9c2 cells (27). In Fig. 6*C*, CRT-overexpressing cells transfected with pGL3-pro-PP2Ac (C3) were

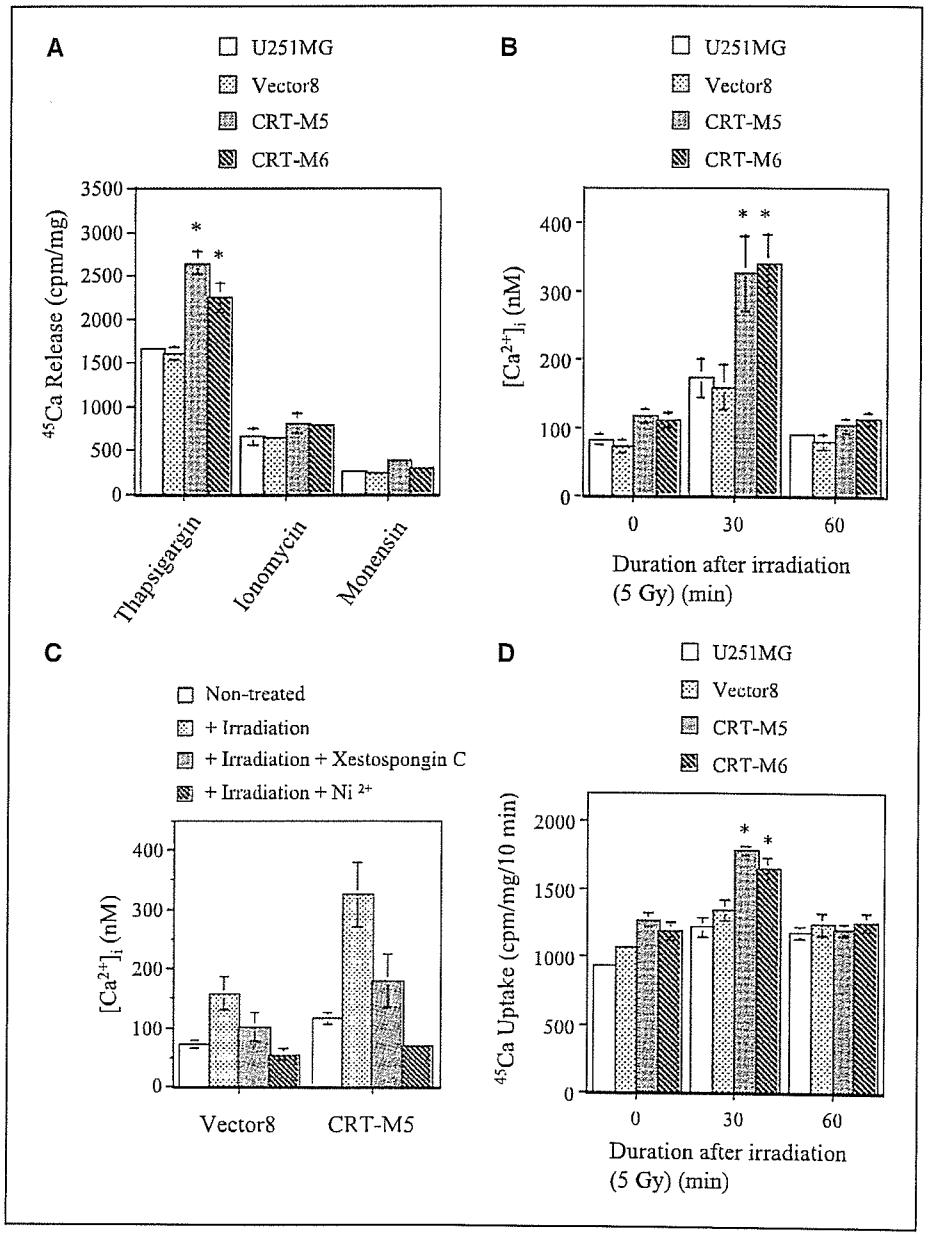

Figure 5. Effect of CRT overexpression on intracellular Ca^{2+} pools and Ca^{2+} responses to irradiation in U251MG cells: *A*, control (U251MG and Vector8) and CRT-overexpressing (CRT-M5 and CRT-M6) cells were cultured with $^{45}Ca^{2+}$ (1 μCi/mL) for 48 hours, then detached from the culture dish and resuspended in Ca^{2+}-free EBSS. Cell suspensions were preincubated at 37°C for 3 minutes, and sequentially stimulated with thapsigargin (0.1 μmol/L), ionomycin (2 μmol/L), and monensin (2 μmol/L). The cell suspensions were collected 5 minutes after the addition of each reagent and centrifuged. The radioactivity released from the cells was measured in the supernatant. Cell pellets were lysed and protein amounts were determined using a BCA assay kit (Pierce). *Columns*, mean of the cpm subtracted from those recovered in the preceding collection, and normalized to the protein in the corresponding cell pellets; *bars*, SD. *, $P < 0.01$ versus U251MG or Vector8 cells treated with thapsigargin. *B*, control and CRT-overexpressing cells were treated with γ-irradiation (5 Gy). $[Ca^{2+}]_i$ was measured after the periods indicated using Fura2-AM as described in Materials and Methods. *Columns*, mean of at least four experiments; *bars*, SD. *, $P < 0.01$ versus U251MG or Vector8 cells at 30 minutes after the irradiation. *C*, control (Vector8) and CRT-overexpressing (CRT-M5) cells were pretreated with or without xestospongin C (5 mmol/L) or Ni^{2+} (5 mmol/L) for 5 minutes, then treated with γ-irradiation (5 Gy). $[Ca^{2+}]_i$ was measured at 30 minutes after the irradiation using Fura2-AM as described above. *Columns*, mean of at least four experiments; *bars*, SD. *, $P < 0.01$ versus Vector8 cells at 30 minutes after the irradiation. **, $P < 0.01$ versus CRT-M5 cells at 30 minutes after the irradiation. *D*, control and CRT-overexpressing cells were treated with γ-irradiation (5 Gy). Then, cells were incubated for 10 minutes with $^{45}Ca^{2+}$ (5 μCi/mL) at the periods indicated after irradiation. After washing with EBSS, the cells were harvested and $^{45}Ca^{2+}$ uptake was measured as described in Materials and Methods. *Columns*, mean of three independent experiments; *bars*, SD. *, $P < 0.01$ versus U251 MG or Vector8 cells at 30 minutes after the irradiation.

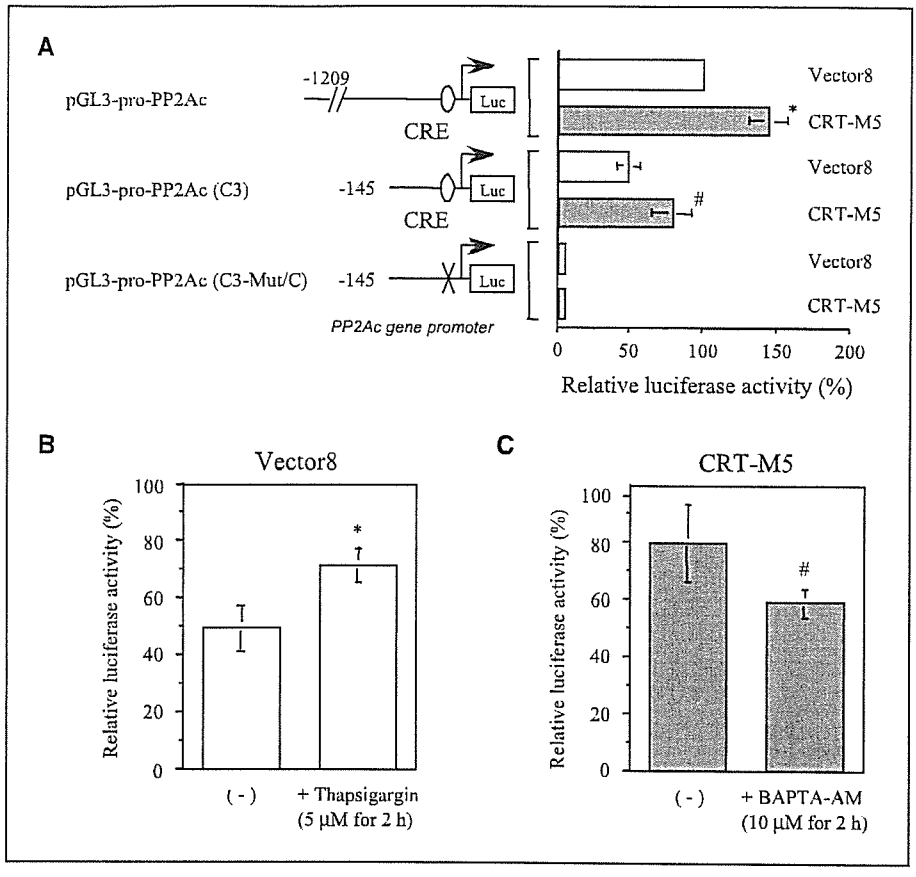

Figure 6. The promoter activity of the *PP2Acα* gene is increased in CRT-overexpressing cells through CRE, and is regulated via altered Ca^{2+} homeostasis. *A, left,* schematic representation of luciferase vector constructs for the rat PP2Acα promoter [i.e., pGL3-pro-PP2Ac, pGL3-pro-PP2Ac (C3), and pGL3-pro-PP2Ac (C3-Mut/C)]. Each luciferase vector construct was generated as described in Materials and Methods. The CRE site (−26) was mutated in pGL3-pro-PP2Ac (C3-Mut/C). *Right,* luciferase activity of the vector constructs for the *PP2Acα* gene promoter in control and CRT-overexpressing cells. The cells were transiently transfected with the PP2Acα promoter-luciferase gene fusion plasmids. After 24 hours of transfection, luciferase activity was assayed with cellular extracts as described in Materials and Methods. *Columns,* mean of at least three experiments; *bars,* SD. *, $P < 0.01$ versus Vector8 cells transfected with pGL3-pro-PP2Ac. #, $P < 0.01$ versus Vector8 cells transfected with pGL3-pro-PP2Ac (C3). Control and CRT-overexpressing cells were transiently transfected with pGL3-pro-PP2Ac (C3). After 24 hours of transfection, control cells were treated with 5 μmol/L thapsigargin for 2 hours (*B*) and CRT-overexpressing cells were treated with 10 μmol/L BAPTA-AM for 2 hours (*C*). Then, luciferase activity was assayed with cell nuclear extracts as described in Materials and Methods. *Columns,* mean of at least three experiments; *bars,* SD. *, $P < 0.05$ versus untreated Vector8 cells. #, $P < 0.05$ versus untreated CRT-M5 cells.

treated with or without BAPTA-AM (10 μmol/L for 2 hours), and then the luciferase activity was assayed as described above. The results showed that the activity of the PP2Acα promoter was down-regulated in CRT-overexpressing cells by the decrease of $[Ca^{2+}]_i$ with BAPTA-AM treatment. Taken together, these results indicate that the activity of the PP2Acα promoter was regulated by $[Ca^{2+}]_i$ through CRE, and overexpression of CRT up-regulates the promoter activity through the altered homeostasis of Ca^{2+} in U251MG cell.

Discussion

In the present study, we focused on functions of endoplasmic reticulum chaperones in malignant gliomas to obtain a new perspective for therapy. To evaluate the association between radiosensitivity and the expression of the molecular chaperones in the endoplasmic reticulum, we used three cultured glia-derived cell lines, i.e., two glioblastoma cell lines (U251MG and T98G) and a neuroglioma cell line (H4). We found that H4 cells were more radiosensitive than U251MG and T98G cells, and the expression level of CRT was specifically higher in H4 than in U251MG or T98G cells (Fig. 1*A* and *B*). These findings suggested that the expression level of CRT seems to be related with radiosensitivity in gliomas. Although the expression of CRT is induced by radiation (34, 35), the function of CRT in radiosensitivity is not well understood. To investigate the significance of CRT in radiosensitivity, we established a CRT-overexpressing cell line using U251MG, and examined the effect of the overexpression on the radiosensitivity. It was found that CRT-overexpressing cells showed greater radiosensitivity than control cells, and enhanced radiation-induced apoptosis.

Radiation-induced apoptosis is controlled by various mechanisms, such as the p53 status, the Bcl-2 gene family, the caspase pathways, and so forth (3). Zhao et al. (36) reported that the DNase activation pathway through p53 and Ca^{2+}-mediated DNase γ pathway were involved in the regulation of radiation-induced apoptosis in Molt-4 cells. However, in U251MG cells, the enhancement of radiation-induced apoptosis by CRT may not be due to a p53-dependent mechanism, because of the mutation in the *p53* gene (37). On the other hand, apoptosis is regulated by several signaling pathways, including the mitogen-activated protein kinases and Akt pathways (38). The Akt signaling pathway is an important cell survival and antiapoptotic signal in radiation-induced apoptosis (39, 40). In this study, we found that the pathway was significantly suppressed in the CRT-overexpressing cells after γ-irradiation. Moreover, we found that the expression of PP2Acα was significantly increased in overexpressing cells compared with control cells. PP2A is known to modulate the activities of several kinases, and is responsible for the dephosphorylation and inactivation of Akt (20, 31). Therefore, these results suggest that Akt signaling was suppressed by the up-regulation of PP2Acα expression in CRT-overexpressing cells treated with γ-irradiation.

The Ca^{2+} concentration of the endoplasmic reticulum or cytoplasm is thought to be a key determinant of radiation-induced apoptosis (9, 11). CRT is a Ca^{2+}-binding molecular chaperone in the endoplasmic reticulum and is involved in the regulation of intracellular Ca^{2+} homeostasis and endoplasmic reticulum Ca^{2+} storage capacity (16). In this study, we found that,

in CRT-overexpressing cells, the thapsigargin-sensitive Ca^{2+} pool was increased, and the levels of $[Ca^{2+}]_i$ and Ca^{2+} influx from the extracellular spaces were both up-regulated, especially after ionizing irradiation. This indicated that CRT overexpression significantly influenced the regulatory mechanism of Ca^{2+} homeostasis in U251MG cells, although the precise mechanism of CRT action has not yet been fully clarified. In addition, we found that the gene promoter of PP2Acα was regulated through the change in $[Ca^{2+}]_i$ (Fig. 6*B* and *C*). These results strongly suggest a mechanical link between down-regulated Akt signaling and altered Ca^{2+} homeostasis in CRT-overexpressing cells, and it is consistent with our finding that the antiapoptotic activity of Akt is down-regulated by Ca^{2+} in myocardiac H9c2 cells (27).

Concerning CRT and apoptosis, Nakamura et al. (10) reported that overexpression of CRT resulted in an increase in the sensitivity of HeLa cells to both thapsigargin- and staurosporine-induced apoptosis. The authors suggested that overexpression of CRT affects the communication between the endoplasmic reticulum and mitochondria to increase the sensitivity to apoptosis via the altered Ca^{2+} homeostasis, and this has been supported by the study of Arnaudeau et al. (41). We also reported that overexpression of CRT influences the function of SERCA2a under oxidative stress, leading to an alteration of Ca^{2+} homeostasis (42) and to enhanced susceptibility to apoptosis (20, 21). These findings suggest that the expression level of CRT is well correlated with the susceptibility to apoptosis. In contrast, overexpression of CRT provided resistance to oxidant-induced cell death in renal epithelial LLC-PK1 cells treated with iodoacetamide (43), *tert*-butylhydroperoxide (44), or hydrogen peroxide (45). In the neuroblastoma × glioma hybrid cell line NG-108-15, suppression of CRT by an antisense oligonucleotide increased sensitivity to ionomycin-induced cytotoxicity (46, 47). The function of CRT in the regulation of apoptosis may differ in specific cell types, and is still controversial. Although almost all studies suggest regulatory functions of CRT in the susceptibility to apoptosis, further investigation is required to clarify the relevance to CRT in cancer biology.

In conclusion, we found that the expression level of CRT was well correlated with radiosensitivity in glioma cell lines, and CRT modulated the radiosensitivity of glioblastoma cell lines by affecting the cell survival pathway of Akt signaling through alterations of Ca^{2+} homeostasis and responses in the endoplasmic reticulum.

Acknowledgments

Received 11/30/2005; revised 5/23/2006; accepted 6/21/2006.

Grant support: The 21st Century Center of Excellence program from the Ministry of Education, Science, Sports, Culture, and Technology of Japan (T. Kondo and Y. Ihara).

The costs of publication of this article were defrayed in part by the payment of page charges. This article must therefore be hereby marked *advertisement* in accordance with 18 U.S.C. Section 1734 solely to indicate this fact.

We thank Midori Ikezaki and Akiko Emura for technical assistance.

References

1. Grossman SA, Batara JF. Current management of glioblastoma multiforme. Semin Oncol 2004;31:635–44.
2. Souhami L, Seiferheld W, Brachman D, et al. Randomized comparison of stereotactic radiosurgery followed by conventional radiotherapy with carmustine to conventional radiotherapy with carmustine for patients with glioblastoma multiforme: report of Radiation Therapy Oncology Group 93-05 protocol. Int J Radiat Oncol Biol Phys 2004;60:853–60.
3. Rupnow BA, Knox SJ. The role of radiation-induced apoptosis as a determinant of tumor responses to radiation therapy. Apoptosis 1999;4:115–43.
4. Zhivotovsky B, Joseph B, Orrenius S. Tumor radiosensitivity and apoptosis. Exp Cell Res 1999;248:10–7.
5. Tribius S, Pidel A, Casper D. ATM protein expression correlates with radioresistance in primary glioblastoma cells in culture. Int J Radiat Oncol Biol Phys 2001;50: 511–23.
6. Bartussek C, Naumann U, Weller M. Accumulation of mutant p53 (V143A) modulates the growth, clonogenicity, and radiochemosensitivity of malignant glioma cells independent of endogenous p53 status. Exp Cell Res 1999;253:432–9.
7. Rich JN, Hans C, Jones B, et al. Gene expression profiling and genetic markers in glioblastoma survival. Cancer Res 2005;65:4051–8.
8. Scotto C, Deloulme JC, Rousseau D, Chambaz E, Baudier J. Calcium and S100B regulation of p53-dependent cell growth arrest and apoptosis. Mol Cell Biol 1998;18:4272–81.
9. Takahashi K, Inanami O, Kuwabara M. Effects of intracellular calcium chelator BAPTA-AM on radiation-induced apoptosis regulated by activation of SAPK/JNK and caspase-3 in MOLT-4 cells. Int J Radiat Biol 1999;75: 1099–105.
10. Nakamura K, Bossy-Wetzel E, Burns K, et al. Changes in endoplasmic reticulum luminal environment affect cell sensitivity to apoptosis. J Cell Biol 2000; 150:731–40.
11. Pinton P, Ferrari D, Rapizzi E, Di Virgilio F, Pozzan T, Rizzuto R. The Ca^{2+} concentration of the endoplasmic reticulum is a key determinant of ceramide-induced apoptosis: significance for the molecular mechanism of Bcl-2 action. EMBO J 2001;20:2690–701.
12. Mesaeli N, Phillipson C. Impaired p53 expression, function, and nuclear localization in calreticulin-deficient cells. Mol Biol Cell 2004;15:1862–70.
13. Rudner J, Jendrossek V, Belka C. New insights in the role of Bcl-2. Bcl-2 and the endoplasmic reticulum. Apoptosis 2002;7:441–7.
14. Yan J, Khanna KK, Lavin MF. Defective radiation signal transduction in ataxia-telangiectasia cells. Int J Radiat Biol 2000;76:1025–35.
15. Orrenius S, Zhivotovsky B, Nicotera P. Regulation of cell death: the calcium-apoptosis link. Nat Rev Mol Cell Biol 2003;4:552–65.
16. Michalak M, Corbett EF, Mesaeli N, Nakamura K, Opas M. Calreticulin: one protein, one gene, many functions. Biochem J 1999;344:281–92.
17. Johnson S, Michalak M, Opas M, Eggleton P. The ins and outs of calreticulin: from the ER lumen to the extracellular space. Trends Cell Biol 2001;11:122–9.
18. Helenius A, Aebi M. Roles of N-linked glycans in the endoplasmic reticulum. Annu Rev Biochem 2004;73: 1019–49.
19. Holaska JM, Black BE, Love DC, Hanover JA, Leszyk J, Paschal BM. Calreticulin is a receptor for nuclear export. J Cell Biol 2001;152:127–40.
20. Kageyama K, Ihara Y, Goto S, et al. Overexpression of calreticulin modulates protein kinase B/Akt signaling to promote apoptosis during cardiac differentiation of cardiomyoblast H9c2 cells. J Biol Chem 2002;277:19255–64.
21. Ihara Y, Urata Y, Goto S, Kondo T. Role of calreticulin in the sensitivity of myocardiac H9c2 cells to oxidative stress caused by hydrogen peroxide. Am J Physiol Cell Physiol 2006;290:C208–21.
22. Brondani Da Rocha A, Regner A, Grivicich I, et al. Radioresistance is associated to increased Hsp70 content in human glioblastoma cell lines. Int J Oncol 2004;25:777–85.
23. Gavrieli Y, Sherman Y, Ben-Sasson SA. Identification of programmed cell death in situ via specific labeling of nuclear DNA fragmentation. J Cell Biol 1992;119:493–501.
24. Gaussen A, Legal JD, Beron-Gaillard N, et al. Radiosensitivity of human normal and tumoral thyroid cells using fluorescence *in situ* hybridization and clonogenic survival assay. Int J Radiation Oncol Biol Phys 1999;44:683–91.
25. Kitamura K, Mizuno Y, Sasaki A, Yasui A, Tsuiki S, Kikuchi K. Molecular cloning and sequence analysis of cDNA for the catalytic subunit 1α of rat kidney type 1 protein phosphatase, and detection of the gene expression at high levels in hepatoma cells and regenerating livers as compared with rat livers. J Biochem (Tokyo) 1991;109:307–10.
26. Kitagawa Y, Tahira T, Ikeda I, et al. Molecular cloning of cDNA for the catalytic subunit of rat liver type 2A protein phosphatase, and detection of high levels of expression of the gene in normal and cancer cells. Biochim Biophys Acta 1998;951:123–9.
27. Yasuoka C, Ihara Y, Ikeda S, Miyahara Y, Kondo T, Kohno S. Antiapoptotic activity of Akt is down-regulated by Ca^{2+} in myocardiac H9c2 cells. Evidence of Ca^{2+}-dependent regulation of protein phosphatase 2Ac. J Biol Chem 2004;279:51182–92.
28. Coffer PJ, Jin J, Woodgett JR. Protein kinase B (c-Akt): a multifunctional mediator of phosphatidylinositol 3-kinase activation. Biochem J 1998;335:1–13.
29. Contessa JN, Hampton J, Lammering G, et al. Ionizing radiation activates Erb-B receptor dependent Akt and p70 S6 kinase signaling in carcinoma cells. Oncogene 2002;21:4032–41.
30. Zingg D, Riesterer O, Fabbro D, Glanzmann C, Bodis S, Pruschy M. Differential activation of the phosphatidylinositol 3′-kinase/Akt survival pathway by ionizing radiation in tumor and primary endothelial cells. Cancer Res 2004;64:5398–406.
31. Millward TA, Zolnierowicz S, Hemmings BA. Regulation of protein kinase cascades by protein phosphatase 2A. Trends Biochem Sci 1999;24:186–91.
32. Jayaraman T, Marks AR. T cells deficient in inositol 1,4,5-trisphosphate receptor are resistant to apoptosis. Mol Cell Biol 1997;17:3005–12.
33. Kurebayashi N, Ogawa Y. Depletion of Ca^{2+} in the sarcoplasmic reticulum stimulates Ca^{2+} entry into mouse skeletal muscle fibres. J Physiol 2001;533:185–99.
34. Ramsamooj P, Notario V, Dritschilo A. Enhanced expression of calreticulin in the nucleus of radioresistant squamous carcinoma cells in response to ionizing radiation. Cancer Res 1995;55:3016–21.

35. Prasad SC, Soldatenkov VA, Kuettel MR, Thraves PJ, Zou X, Dritschilo A. Protein changes associated with ionizing radiation-induced apoptosis in human prostate epithelial tumor cells. Electrophoresis 1999;20:1065–74.
36. Zhao QL, Kondo T, Noda A, Fujiwara Y. Mitochondrial and intracellular free-calcium regulation of radiation-induced apoptosis in human leukemic cells. Int J Radiat Biol 1999;75:493–504.
37. Van Meir EG, Kikuchi T, Tada M, et al. Analysis of the p53 gene and its expression in human glioblastoma cells. Cancer Res 1994;54:649–52.
38. Belka C, Jendrossek V, Pruschy M, Vink S, Verheij M, Budach W. Apoptosis-modulating agents in combination with radiotherapy—current status and outlook. Int J Radiation Oncol Biol Phys 2004;58:542–54.
39. Tan J, Hallahan DE. Growth factor-independent activation of protein kinase B contributes to the inherent resistance of vascular endothelium to radiation-induced apoptosis response. Cancer Res 2003;63:7663–7.
40. McKenna WG, Muschel RJ, Gupta AK, Hahn SM, Bernhard EJ. The Ras signal transduction pathway and its role in radiation sensitivity. Oncogene 2003;22:5866–75.
41. Arnaudeau S, Frieden M, Nakamura K, Castelbou C, Michalak M, Demaurex N. Calreticulin differentially modulates calcium uptake and release in the endoplasmic reticulum and mitochondria. J Biol Chem 2002;277:46696–705.
42. Ihara Y, Kageyama K, Kondo T. Overexpression of calreticulin sensitizes SERCA2a to oxidative stress. Biochem Biopys Res Commun 2005;329:1343–9.
43. Liu H, Bowes RC III, van de Water B, Sillence C, Nagelkerke JF, Stevens JL. Endoplasmic reticulum chaperones GRP78 and calreticulin prevent oxidative stress, Ca^{2+} disturbances, and cell death in renal epithelial cells. J Biol Chem 1997;272:21751–9.
44. Liu H, Miller E, van de Water B, Stevens JL. Endoplasmic reticulum stress proteins block oxidant-induced Ca^{2+} increases and cell death. J Biol Chem 1998;273:12858–62.
45. Hung CC, Ichimura T, Stevens JL, Bonventre JV. Protection of renal epithelial cells against oxidative injury by endoplasmic reticulum stress preconditioning is mediated by ERK1/2 activation. J Biol Chem 2003;278:29317–26.
46. Liu N, Fine RE, Simons E, Johnson RJ. Decreasing calreticulin expression lowers the Ca^{2+} response to bradykinin and increases sensitivity to ionomycin in NG-108-15 cells. J Biol Chem 1994;269:28635–9.
47. Johnson RJ, Liu N, Shanmugaratnam J, Fine RE. Increased calreticulin stability in differentiated NG-108-15 cells correlates with resistance to apoptosis induced by antisense treatment. Brain Res Mol Brain Res 1998;53:104–11.

Long term smoking with age builds up excessive oxidative stress in bronchoalveolar lavage fluid

K Nagai, T Betsuyaku, T Kondo, Y Nasuhara and M Nishimura

Thorax 2006;61;496-502; originally published online 14 Mar 2006;
doi:10.1136/thx.2005.049148

SMOKING

Long term smoking with age builds up excessive oxidative stress in bronchoalveolar lavage fluid

K Nagai, T Betsuyaku, T Kondo, Y Nasuhara, M Nishimura

Thorax 2006;61:496–502. doi: 10.1136/thx.2005.049148

See end of article for authors' affiliations

Correspondence to: Dr T Betsuyaku, First Department of Medicine, Hokkaido University School of Medicine, N-15, W-7, Kita-ku, Sapporo, Japan 060-8638; bytomoko@med.hokudai.ac.jp

Received 7 July 2005
Accepted 17 January 2006
Published Online First 14 March 2006

Background: Epithelial lining fluid plays a critical role in protecting the lung from oxidative stress, in which the oxidised status may change by ageing, smoking history, and pulmonary emphysema.
Methods: Bronchoalveolar lavage (BAL) was performed on 109 young and older subjects with various smoking histories. The protein carbonyls, total and oxidised glutathione were examined in BAL fluid.
Results: By Western blot analysis, the major carbonylated protein in the BAL fluid was sized at 68 kDa, corresponding to albumin. The amount of carbonylated albumin per mg total albumin in BAL fluid was four times higher in older current smokers and three times higher in older former smokers than in age matched non-smokers ($p<0.0001$, $p=0.0003$, respectively), but not in young smokers. Total glutathione in BAL fluid was significantly increased both in young ($p=0.006$) and older current smokers ($p=0.0003$) compared with age matched non-smokers. In contrast, the ratio of oxidised to total glutathione was significantly raised (72%) only in older current smokers compared with the other groups. There was no significant difference in these parameters between older smokers with and without mild emphysema.
Conclusions: Oxidised glutathione associated with excessive protein carbonylation accumulates in the lung of older smokers with long term smoking histories even in the absence of lung diseases, but they are not significantly enhanced in smokers with mild emphysema.

The lung is an organ constantly exposed to exogenous oxidants such as cigarette smoke and air pollutants. Epithelial lining fluid (ELF) acts as an interface between the airspace epithelium and the external environment and therefore affords protection against epithelial cell injury.[1] Because the constituents of ELF form the primary targets of inhaled oxidant pollutants and also inflammatory reactive oxygen species (ROS) generated within the alveolar space, the oxidative modifications of certain extracellular targets and their functional consequences have received considerable attention.[2] It is known that protein carbonylation reflects the oxidation of Lys, Arg, or Pro residues in proteins. The content of protein carbonyls is therefore by far the most commonly used marker for protein oxidation.[3]

On the other hand, there are various kinds of extracellular antioxidants in the lungs such as mucin, uric acid, ascorbic acid, α-tocopherol, glutathione, antioxidant enzymes and proteins that are capable of binding metals. Glutathione is a sulfhydryl-containing tripeptide (L-gamma-glutamyl-L-cysteinyl-glycine) that is present in high concentrations in all cells and protects against intracellular oxidants and xenobiotics.[4] Extracellular glutathione can be augmented by cellular sources from respiratory tract epithelial cells and inflammatory cells such as macrophages. The levels of glutathione in ELF are 100-fold higher than in plasma, which may indicate its relative importance among the various antioxidants.[4 5]

The elderly are particularly vulnerable to smoking associated respiratory diseases. Worldwide, the ratio of smokers is still high among the middle aged or elderly population, and they usually have long term smoking histories. Cigarette smoking is a major risk factor for the development of emphysema, and it normally affects patients in the fifth to sixth decade of life. Although an oxidant/antioxidant imbalance has been implicated in the development of emphysema,[6] there is still a large gap in our understanding of the link between the cumulative effects of ageing and decades of continuous smoking on the oxidative stress and antioxidant mechanisms in the lung. Total glutathione is known to be raised in the bronchoalveolar lavage (BAL) fluid of recent young smokers, and the majority (>95%) of the total glutathione is maintained in the reduced state.[5] However, there is a lack of information on the levels and redox state of glutathione in the BAL fluid of older smokers with or without pulmonary emphysema.

We therefore investigated whether chronic smoking induced changes in protein carbonylation and glutathione redox status in BAL fluid differ by age, duration of smoking, or the presence of emphysema. BAL was performed to obtain ELF from lifelong non-smokers as well as young and older smokers with various smoking histories.

METHODS

Subjects

A total of 109 community based asymptomatic volunteers were recruited from the patients in our smoking cessation and non-pulmonary clinics and from the employees and students in our medical school. Most of the subjects had taken part in previous studies in our laboratory.[7 8] The young group (age 20–29 years, n = 39) consisted of 16 lifelong non-smokers and 23 current smokers who had smoked for less than 3 years. The older group (age 37–77 years, n = 70) included seven lifelong non-smokers, 17 former smokers, and 46 current smokers with smoking histories of more than 20 years. Former smokers were arbitrarily defined as people who had quit smoking for at least 1 year. None of the subjects was on regular medication or had a history of asthma or other allergic disorders. All subjects had been free of clinically apparent respiratory infections for the preceding 2 months and had been evaluated by physical examination, chest radiography, and a blood test. After elimination of non-

Abbreviations: BAL, bronchoalveolar lavage; DNP, dinitrophenylhydrazine; ELF, epithelial lining fluid; FEV_1, forced expiratory volume in 1 second; GSH, reduced glutathione; GSSG, glutathione disulfide

eligible subjects, all older former and current smokers were screened for emphysematous changes by high resolution computed tomographic (HRCT) scanning as previously described.[9] Pulmonary function tests were performed in accordance with the standard techniques of the American Thoracic Society. Forced expiratory volume in 1 second (FEV_1) from the flow-volume curve was expressed as a percentage of the predicted value according to the equations of Berglund *et al.*[10]

All of the subjects provided written informed consent and the study was approved by the ethics committee of Hokkaido University School of Medicine.

Sequential BAL

Sequential BAL was performed through a wedged flexible fibreoptic bronchoscope (Olympus BF-B3R, Tokyo, Japan) as described previously.[9] The fluid returned from the first 50 ml aliquot was not used in the study. The remaining lavage fluid was pooled and used as the BAL fluid. Differential cell counts were performed as previously described.[9] The level of total protein in the BAL fluid was determined using a Micro BCA Protein Assay Reagent kit (Pierce Biotech, IL, USA). The level of albumin was quantified by laser nephelometry as described previously.[9] The level of transferrin was measured using the human transferrin enzyme linked immunosorbent assay quantification kit (Bethyl Laboratories Inc, TX, USA).

Assessment of protein carbonyls in BAL fluid

Oxidation of individual BAL fluid proteins was measured by analysis of Western blots according to the method of Shacter *et al.*[11] BAL fluid was derivatised with dinitrophenylhydrazine (DNP) using the OxyBlot Protein Oxidation Detection kit (Chemicon International, Temecula, CA, USA) with slight modification. Briefly, 16 µl of unconcentrated BAL fluid were denatured by adding 3 µl of 20% sodium dodecylsulfate (SDS)-polyacrylamide, derivatised by adding 1 µl 10X DNPH solution, and neutralised by adding 7.5 µl neutralization solution and 1.5 µl 2-mercaptoethanol. Samples were separated by electrophoresis on 10% SDS-polyacrylamide electrophoresis gels. Blots were performed using the anti-DNP antibody and scanned with a GT-9500 scanner (Epson, Nagano, Japan); the intensity of the bands was calculated using NIH Image software (version 1.62). On each blot the recorded total DNP intensity of all bands detected for each lane was divided by that of a standard sample from a representative young non-smoker. The total carbonyl content in the BAL fluid was referred as total DNP units/ml BAL fluid. The assay for the total carbonyl content had an intrabatch coefficient of variation of 12% (n = 7) and an interbatch coefficient of variation of 16% (n = 5).

The molecular masses of albumin and transferrin were determined by Western blotting on the same membrane used for the Oxyblot. Specifically, after the Western blot for carbonyl proteins, the anti-DNP antibody was removed, then incubated with 1:1000 peroxidase conjugated anti-human albumin antibody (DAKO, Glostrup, Denmark) or 1:1000 rabbit anti-human transferrin (Dakocytomation, Glostrup, Denmark) followed by 1:15 000 horseradish peroxidase conjugated goat anti-rabbit antibody (DAKO). Sites of antibody binding were visualised using the ECL^{Plus} Western blotting detection system (Amersham, Aylesbury, UK).

Measurement of total glutathione and glutathione disulfide in BAL fluid

Total glutathione and glutathione disulfide (GSSG), oxidised glutathione, were measured in all samples using a glutathione assay kit (Cayman Chemical Co, MI, USA) as described by Tietze and co-workers.[12] The assays for total glutathione and GSSG had intrabatch coefficients of variation of 3% (n = 12) and 3% (n = 10), respectively, and interbatch coefficients of variation of 6% (n = 10) and 13% (n = 8), respectively.

Statistical analyses

Differences between the two means were performed with a two tailed unpaired Student's *t* test using Statview Software (SAS Institute Inc, NC, USA). More than two means were compared by analysis of variance followed by the Games-Howell method using SAS software Version 8.2 (SAS Institute Inc). A value of $p<0.05$ was considered to be statistically significant. The results are reported as standard error of the mean (SE).

RESULTS

Characteristics of subjects

Clinical characteristics and pulmonary function data for the subjects are summarised in table 1. Emphysema, as detected on CT scans, was less than 25% of the total lung area in most subjects categorised in the emphysema groups. There was no difference in the number of cigarettes smoked per day between young and older current smokers.

BAL findings

BAL findings are shown in table 2. The total protein, albumin, and transferrin levels in BAL fluid from young smokers were significantly lower than those from young non-smokers. There were no differences in the levels of total protein, albumin, and transferrin in BAL fluid among older groups. The numbers of total cells and macrophages in BAL fluid were significantly increased in current smokers

Table 1 Characteristics of subjects

	Young		Older				
			Former smokers		Current smokers		
	Non-smokers	Current smokers	Non-smokers	No emphysema	Emphysema	No emphysema	Emphysema
No of subjects	16	23	7	7	10	21	25
Age (years)	23 (1)	23 (0)	63 (3)	65 (2)	59 (3)	57 (2)	61 (2)
Cigarettes/day	0	20 (1)	0	0	0	27 (5)	25 (4)
Pack-years	0	5 (1)	0	35 (10)	41 (7)	55 (5)	45 (4)
VC (% pred)	97 (3)	96 (3)	122 (8)	125 (3)	110 (3)†	110 (4)	110 (4)
FEV_1 (% pred)	83 (3)	88 (3)	124 (8)	129 (5)	97 (5)†	101 (5)	92 (4)‡
FEV_1/FVC (%)	91 (2)	88 (2)	84 (2)	80 (2)	73 (3)*	79 (2)	70 (2)*‡

VC, vital capacity; FEV_1, forced expiratory volume in 1 second; FVC, forced vital capacity.
Data are expressed as mean (SE).
*Significantly different from older non-smokers ($p<0.05$).
†Significantly different from older former smokers without emphysema ($p<0.05$).
‡Significantly different from older current smokers without emphysema ($p<0.05$).

Table 2 BAL fluid findings

	Young		Older				
				Former smokers		Current smokers	
	Non-smokers	Current smokers	Non-smokers	No emphysema	Emphysema	No emphysema	Emphysema
Recovery rate (%)	74 (4)	64 (3)*	71 (4)	54 (5)	33 (5)† ‡	50 (4)†	33 (5)†§
Albumin (mg/l)	47 (7)	33 (3)*	55 (9)	57 (11)	59 (11)	32 (2)	50 (10)
Total protein (mg/l)	116 (14)	92 (7)*	160 (22)	128 (28)	210 (44)	111 (10)	142 (13)
Transferrin (mg/l)	3.8 (0.4)	2.9 (0.2)*	7.4 (2.0)	4.3 (1.2)	4.5 (1.1)	3.9 (0.4)	3.6 (0.3)
Total cells ($\times10^{-4}$/ml)	8.1 (0.9)	20.1 (2.2)*	13.4 (1.3)	9.6 (2.4)	10.5 (3.4)	27.3 (4.3)†	36 (8.2)†
Macrophages ($\times10^{-4}$/ml)	6.9 (0.9)	19.5 (2.1)*	10.8 (1.3)	8.0 (1.9)	8.4 (2.4)	25.9 (4.1)†	32.9 (8.0)†
Neutrophils ($\times10^{-4}$/ml)	0.20 (0.05)	0.24 (0.08)	0.04 (0.01)	0.05 (0.01)	0.06 (0.02)	0.62 (0.45)	0.59 (0.25)

Data are expressed as mean (SE).
*Significantly different from young non-smokers ($p<0.05$).
†Significantly different from older non-smokers ($p<0.05$).
‡Significantly different from older former smokers without emphysema ($p<0.05$).
§Significantly different from older smokers without emphysema ($p<0.05$).

compared with non-smokers, both in young and older groups. The percentage of macrophages and neutrophils in BAL fluid did not differ between young and older current smokers.

Total protein carbonyls in BAL fluid

The immunoblot analysis demonstrated a major carbonyl protein band for all of the subjects with a molecular weight of 68 kDa (fig 1A and B) and a faint band of 80 kDa for most of the subjects. These bands were speculated to be albumin and transferrin, respectively, based on removal of the anti-DNP antibody followed by Western blotting with antibodies against human albumin or human transferrin (fig 2). As shown in fig 3, the total DNP in units/ml BAL fluid from older current and former smokers was significantly higher than in lifelong non-smokers of the same age (1.72 (0.18) and 1.81 (0.24) *v* 0.7 (0.29) unit/ml; $p = 0.0028$ and $p = 0.0078$, respectively). In contrast, no difference was found in the total DNP units/ml BAL fluid between non-smokers and current smokers among the young subjects (1.05 (0.14) *v* 1.0 (0.09) units/ml, $p = 0.82$). There was also no difference between former smokers with and without emphysema (2.16 (0.34) *v* 1.32 (0.22) units/ml, $p = 0.08$) or between current smokers with and without emphysema (2.00 (0.31) *v* 1.44 (0.14) units/ml, $p = 0.15$).

Albumin carbonylation in BAL fluid

To focus on the carbonylation of albumin, DNP units of the 68-kDa band (corresponding to albumin) were quantified. The value was normalised according to the concentration of albumin in the BAL fluid (fig 4). The ratio of carbonylated albumin per mg total albumin was four times higher in older current smokers and three times higher in older former smokers than in age matched lifelong non-smokers (fig 4). In contrast, there was no difference in the ratio of albumin carbonylation in BAL fluid between young smokers and non-smokers ($p = 0.21$). In both current and former smokers there was no difference in the ratio of albumin carbonylation between the subjects with and without emphysema.

Total glutathione and GSSG in BAL fluid

Total glutathione was detected in unconcentrated BAL fluid for all subjects (fig 5). The concentration of total glutathione in BAL fluid was significantly increased in smokers compared with non-smokers, even in young subjects (3.11 (0.4) *v* 1.17 (0.33) μg/ml, $p = 0.006$). It was also significantly increased in older current smokers compared with age matched non-smokers and former smokers (2.64 (0.34) *v* 0.89 (0.19) and 0.88 (0.29) μg/ml, $p = 0.0003$ and $p = 0.0014$, respectively). In contrast, the level of GSSG was markedly raised only in older current smokers (1.38 (0.2) μg/ml) and was mostly

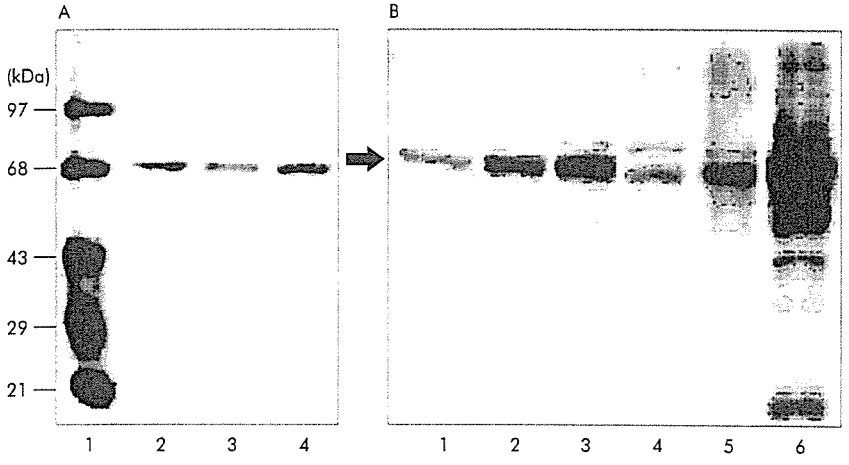

Figure 1 Representative Western blots of oxidised protein in BAL fluid. (A) Representative Western blots from young subjects. Lane 1, molecular weight protein standards in which the second band from the top (68 kDa) is bovine serum albumin; lane 2, a young non-smoker; lane 3, a young current smoker; lane 4, a young non-smoker which was used as a standard for each blot. (B) Representative blots from older subjects. Lane 1, standard BAL sample also shown in lane 4 of (A); lanes 2 and 3, older current smokers without emphysema; lane 4, older non-smoker; lanes 5 and 6, older current smokers with emphysema.

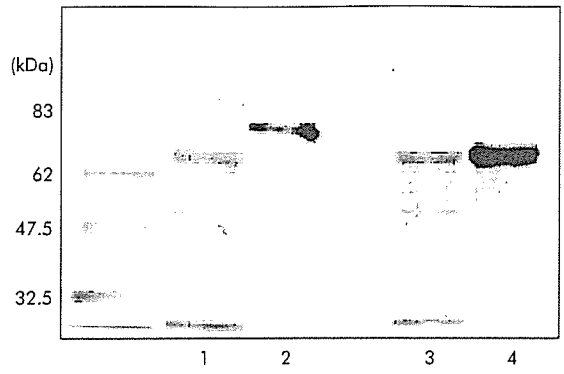

Figure 2 Immunoblots for transferrin and albumin in BAL fluid. After removal of the anti-DNP antibody, Western blotting was carried out on the same membrane. Lanes 1 and 3, anti-DNP antibody; lane 2, anti-human transferrin antibody; lane 4, anti-human albumin antibody. The positions of the molecular weight standards are shown on the left.

under the detection limit in the other groups (fig 6). No significant difference was observed between former or current smokers with and without emphysema either in the level of total glutathione in BAL fluid (former smokers: 1.15 (0.47) *v* 0.49 (0.12) μg/ml, p = 0.23; current smokers: 2.78 (0.55) *v* 2.46 (0.38) μg/ml, p = 0.64) or in the level of GSSG in BAL fluid (former smokers: 0.28 (0.13) *v* 0.09 (0.05) μg/ml, p = 0.27; current smokers: 1.48 (0.38) *v* 1.28 (0.26) μg/ml, p = 0.67, respectively). The ratio of GSSG per total glutathione in older current smokers was as high as 0.72 and was significantly higher than in the other groups (fig 7).

DISCUSSION

In this study we have shown that older smokers with a long term history of smoking have excessive protein carbonyls and accumulate GSSG in BAL fluid, indicating that endogenous antioxidant defences are overwhelmed. Based on the number of cigarettes smoked per day, the amount of exogenous ROS from cigarette smoke was similar for all current smokers regardless of their age; however, the young and older current smokers undoubtedly developed different levels of oxidative stress in the lungs. On the other hand, ageing alone did not affect the level of protein carbonyls, total glutathione, or GSSG in BAL fluid.

The reaction of ROS with proteins results in the formation of carbonyl groups on amino acid residues. Oxidative stress overwhelming the antioxidant defence of the lung may lead to lung injury through a variety of mechanisms including lipid peroxidation of epithelial cell membranes.[13 14] Total protein carbonyls are reportedly increased in the BAL fluid from patients with acute respiratory distress syndrome,[15] idiopathic pulmonary fibrosis, sarcoidosis, asbestosis,[16] and cystic fibrosis.[17] Notably, we found in this study that the level of total protein carbonyls in BAL fluid was raised not only in older current smokers but also in older former smokers despite not smoking for at least a year, indicating that the mechanisms responsible for increased protein carbonyls associated with smoking persist after cessation.

To clarify how protein oxidation participates in pathogenic processes, it will be important to identify the organ and/or disease specific proteins that are most susceptible to oxidative modification and the functional effects of their oxidation. Albumin and transferrin in the serum of mice and albumin and α_1-macroglobulin in the serum of rats accrue significant levels of carbonylation.[18] In the plasma of humans, albumin, fibrinogen, and both fibrinogen γ-chain and α_1-antitrypsin precursors are major targets for carbonylation in uraemia,[19] lung cancer,[20] and Alzheimer's disease,[21] respectively. We report here for the first time that the oxidation of albumin—the most abundant protein in BAL fluid—mostly accounts for excessive total protein carbonylation in older smokers. It is plausible that albumin in BAL fluid from older current smokers may lose its functional efficiency as a consequence of carbonylation because oxidative modifications of albumin reportedly attenuate its antioxidative capacity.[22]

Glutathione also functions as an extracellular antioxidant of the lungs by preventing the oxidation of functional surfactants and antioxidant enzymes only in its reduced form (GSH).[5 23] GSH inhibits protein carbonyl formation in plasma following exposure to cigarette smoke.[24] Although the concentration of total glutathione in BAL fluid is known to vary between lung diseases, the presence of its oxidised form in BAL fluid has only been studied in asthma,[25] cystic fibrosis,[26] and acute respiratory distress syndrome.[27] In the BAL fluid of acute respiratory distress syndrome patients, a significant portion of the total glutathione is in the oxidised form (GSSG), which is likely to be due to the rapid extracellular oxidation of glutathione.[27]

Although the regulation of glutathione in BAL fluid is poorly understood, we speculate that GSSG accumulates in

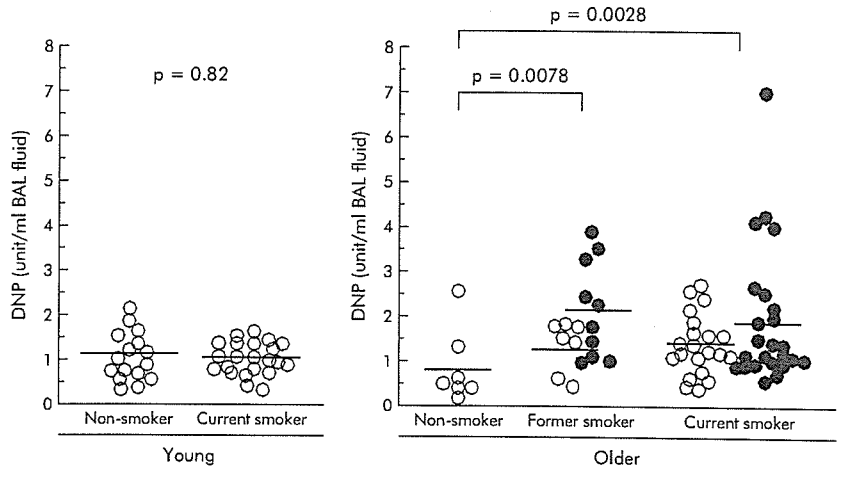

Figure 3 Total DNP units/ml in BAL fluid. Horizontal lines represent mean values of each group. Open circles represent subjects without emphysema; closed circles represent subjects with emphysema. DNP, dinitrophenylhydrazine.

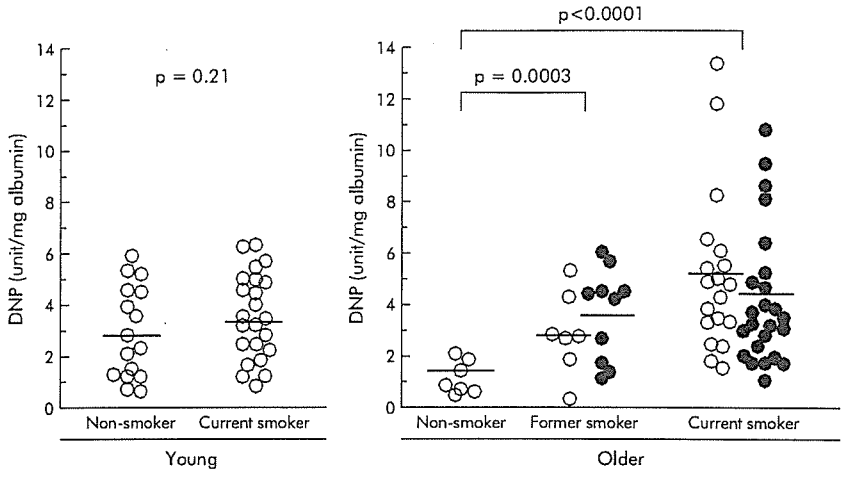

Figure 4 Carbonylated albumin/mg total albumin in BAL fluid. The horizontal lines represent mean values of each group. Open circles represent subjects without emphysema; closed circles represent subjects with emphysema. DNP, dinitrophenylhydrazine.

BAL fluid in older smokers by the following mechanisms. Firstly, the extracellular conversion of GSH into GSSG is accelerated as a result of excessive hydrogen peroxide generated in the ELF by extracellular glutathione peroxidase. Secondly, the efflux of GSSG from the lung cells is increased because of intracellular oxidative stress. Lung cells have many redox regulating enzymes and thiol containing proteins such as thioredoxins or peroxiredoxins that affect the intracellular GSSG/GSH balance.[28–30] When the level of intracellular GSSG increases, the export might be accelerated by adenosine triphosphate binding cassette transporters such as multidrug resistant associated protein I (MRP I).[31] Thirdly, extracellular GSSG catabolism might be impaired due to the attenuation of membrane bound γ-glutamyl transpeptidase activity.[32] Fourthly, protein reactive thiols, which react with GSSG to release GSH, might be reduced in ELF leading to protein mixed disulfide synthesis.[33] Taken together, it is likely that excessive oxidative stress in the lung is causally related to the high level of GSSG in BAL fluid.

Sampling of the ELF by BAL is a common means of studying proteins and investigating their changes in lung diseases. Because of the lack of an appropriate marker for the dilution of lavage fluids (to correct for variable recovery of epithelial lining fluid[34]), we decided not to normalise the data to albumin or urea. Instead, the data were expressed as the concentrations in the lavaged fluid as in our previous studies.[7 8] Despite the difference in the recovery rate of lavage fluid, the level of albumin in the BAL fluid did not differ between the groups (table 2). However, whether the variable rate of recovery may affect the results of comparisons between the groups cannot be determined.

The method and period of storage are also important for evaluating the oxidative status. We used frozen/preserved BAL fluid samples for the assays. Small aliquots of cell free supernatant of BAL fluid were made upon harvest and stored at −70°C to avoid repeated freezing and thawing. It is difficult to directly validate the stability of BAL fluid stored for long periods, but we did not find a significant correlation

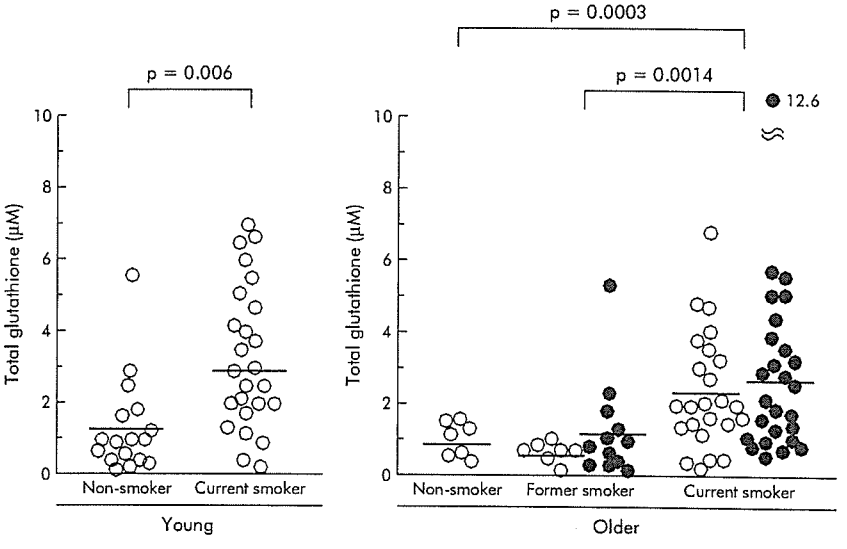

Figure 5 Levels of total glutathione in BAL fluid. The horizontal lines represent mean values of each group. Open circles represent subjects without emphysema; closed circles represent subjects with emphysema.

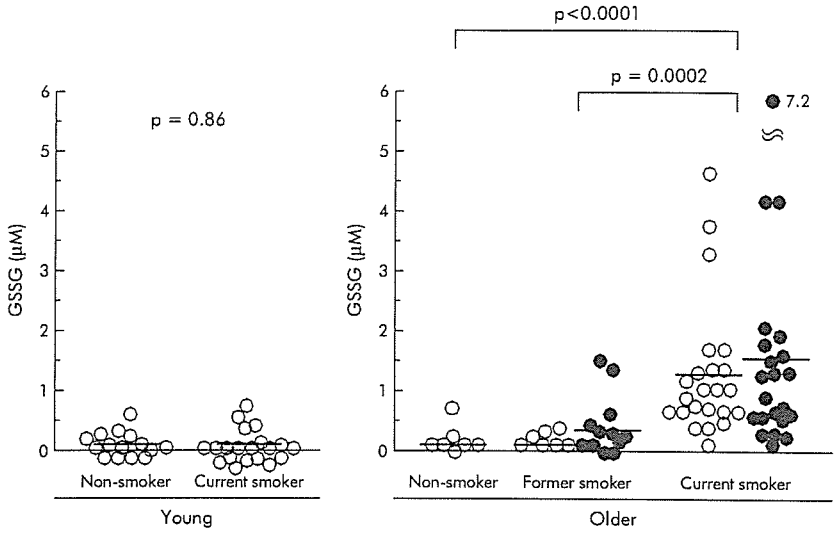

Figure 6 Levels of glutathione disulfide (GSSG) in BAL fluid. The horizontal lines represent mean values of each group. Open circles represent subjects without emphysema; closed circles represent subjects with emphysema.

between storage periods (1–11 years) and the values for each assay for older current smokers (for carbonylated albumin, $n = 40$, $p = 0.73$; for GSSG, $n = 40$, $p = 0.65$). These results imply that markers of oxidative status such as GSSG and carbonylated albumin in BAL fluid are not directly affected by long term storage at −70°C.

This study clearly shows that the effects of smoking on the extracellular redox system differ with age between recent and long term smokers. It should be noted that older smokers are exposed to cigarette smoke over the years while concurrently ageing. Following smoking, the content of glutathione and the ratio of GSH to total glutathione in the whole lung are significantly lower in senescence accelerated mice than in senescence resistant mice.[35] In humans, long term smoking leads to age related decreases in antioxidant activity in alveolar macrophages.[36] We also recently reported a decrease with age in surfactant proteins A and D in the BAL fluid of long term smokers compared with age matched non-smokers, whereas such differences were not observed among young subjects.[7] Increases in several markers of oxidative stress have been reportedly linked to pulmonary diseases such as chronic obstructive pulmonary disease.[14 37–39] It is still not clear whether oxidative stress plays a direct role in the pathogenesis of chronic obstructive pulmonary disease or whether there is more oxidative stress as a result of ageing with long term chronic smoking. To address this issue, we first evaluated oxidative stress and glutathione redox status in BAL fluids collected from more than 100 subjects classified by age, smoking status, and the presence of mild emphysema in this study.

Although we did not observe a significant enhancement associated with the presence of emphysema according to CT scans, it should be noted that the severity of emphysema was classified as low and that the distribution was heterogeneous even in the older smokers classified as having emphysema. We cannot therefore rule out the possibility that the protein carbonyls and/or GSSG might be higher in BAL fluid from individuals with more advanced stages of emphysema.

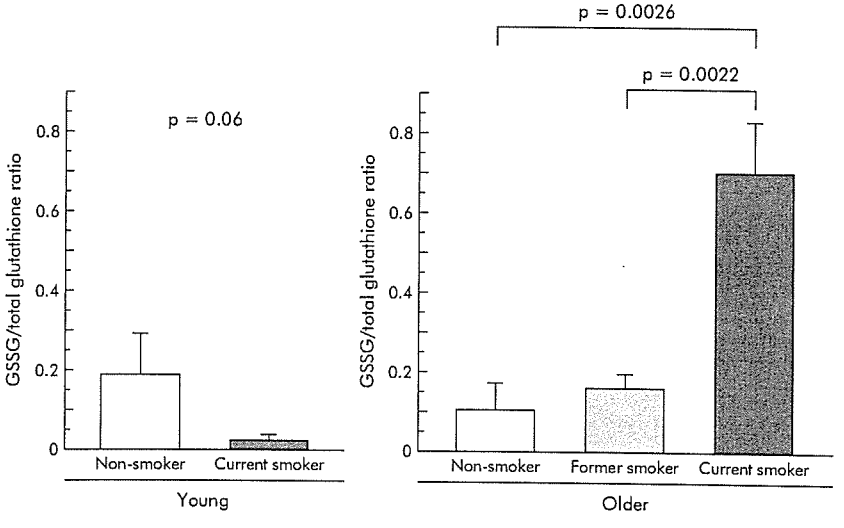

Figure 7 Glutathione disulfide (GSSG)/total glutathione ratio in BAL fluid. Data are mean (SE) values for each group.

Although smoking related diseases are often found in older individuals, it is important to keep in mind that the extracellular antioxidant systems in the lungs of older people have an impaired ability to resist damage from cigarette smoke. Further studies will investigate the functions of GSSG and oxidised proteins in BAL fluid and the potential benefits of antioxidant supplementation for middle aged or elderly smokers.

Authors' affiliations
K Nagai, T Betsuyaku, Y Nasuhara, M Nishimura, First Department of Medicine, Hokkaido University School of Medicine, Sapporo, Japan
T Kondo, Nagasaki University Graduate School of Biomedical Sciences, Nagasaki, Japan

This research was supported by the Respiratory Failure Research Group of the Ministry of Health, Labor, and Welfare of Japan and scientific research grants from the Ministry of Education, Science, Culture and Sports of Japan (13470125 to MN and 14570532 to TB).

Competing interests: none declared.

REFERENCES

1 **Mudway IS**, Kelly FJ. Modeling the interactions of ozone with pulmonary epithelial lining fluid antioxidants. *Toxicol Appl Pharmacol* 1998;**148**:91–100.
2 **Davies KJ**. Protein damage and degradation by oxygen radicals. I. General aspects. *J Biol Chem* 1987;**262**:9895–901.
3 **Dalle-Donne I**, Giustarini D, Colombo R, *et al*. Protein carbonylation in human diseases. *Trends Mol Med* 2003;**9**:169–76.
4 **Rahman I**, MacNee W. Lung glutathione and oxidative stress: implications in cigarette smoke-induced airway disease. *Am J Physiol* 1999;**277**:L1067–88.
5 **Cantin AM**, North SL, Hubbard RC, *et al*. Normal alveolar epithelial lining fluid contains high levels of glutathione. *J Appl Physiol* 1987;**63**:152–7.
6 **MacNee W**, Rahman I. Is oxidative stress central to the pathogenesis of chronic obstructive pulmonary disease? *Trends Mol Med* 2001;**7**:55–62.
7 **Betsuyaku T**, Kuroki Y, Nagai K, *et al*. Effects of ageing and smoking on SP-A and SP-D levels in bronchoalveolar lavage fluid. *Eur Respir J* 2004;**24**:964–70.
8 **Nagai K**, Betsuyaku T, Ito Y, *et al*. Decrease of vascular endothelial growth factor in macrophages from long-term smokers. *Eur Respir J* 2005;**25**:626–33.
9 **Yoshioka A**, Betsuyaku T, Nishimura M, *et al*. Excessive neutrophil elastase in bronchoalveolar lavage fluid in subclinical emphysema. *Am J Respir Crit Care Med* 1995;**152**:2127–32.
10 **Berglund E**, Birath G, Bjure J, *et al*. Spirometric studies in normal subjects. I. Forced expirograms in subjects between 7 and 70 years of age. *Acta Med Scand* 1963;**173**:185–91.
11 **Shacter E**, Williams JA, Lim M, *et al*. Differential susceptibility of plasma proteins to oxidative modification: examination by western blot immunoassay. *Free Radic Biol Med* 1994;**17**:429–37.
12 **Tietze F**. Enzymic method for quantitative determination of nanogram amounts of total and oxidized glutathione: applications to mammalian blood and other tissues. *Anal Biochem* 1969;**27**:502–22.
13 **Altuntas I**, Dane S, Gumustekin K. Effects of cigarette smoking on lipid peroxidation. *J Basic Clin Physiol Pharmacol* 2002;**13**:69–72.
14 **Rahman I**, van Schadewijk AA, Crowther AJ, *et al*. 4-Hydroxy-2-nonenal, a specific lipid peroxidation product, is elevated in lungs of patients with chronic obstructive pulmonary disease. *Am J Respir Crit Care Med* 2002;**166**:490–5.
15 **Lenz AG**, Jorens PG, Meyer B, *et al*. Oxidatively modified proteins in bronchoalveolar lavage fluid of patients with ARDS and patients at-risk for ARDS. *Eur Respir J* 1999;**13**:169–74.
16 **Lenz AG**, Costabel U, Maier KL. Oxidized BAL fluid proteins in patients with interstitial lung diseases. *Eur Respir J* 1996;**9**:307–12.
17 **Kettle AJ**, Chan T, Osberg I, *et al*. Myeloperoxidase and protein oxidation in the airways of young children with cystic fibrosis. *Am J Respir Crit Care Med* 2004;**170**:1317–23.
18 **Jana CK**, Das N, Sohal RS. Specificity of age-related carbonylation of plasma proteins in the mouse and rat. *Arch Biochem Biophys* 2002;**397**:433–9.
19 **Himmelfarb J**, McMonagle E. Albumin is the major plasma protein target of oxidant stress in uremia. *Kidney Int* 2001;**60**:358–63.
20 **Pignatelli B**, Li CQ, Boffetta P, *et al*. Nitrated and oxidized plasma proteins in smokers and lung cancer patients. *Cancer Res* 2001;**61**:778–84.
21 **Choi J**, Malakowsky CA, Talent JM, *et al*. Identification of oxidized plasma proteins in Alzheimer's disease. *Biochem Biophys Res Commun* 2002;**293**:1566–70.
22 **Bourdon E**, Loreau N, Blache D. Glucose and free radicals impair the antioxidant properties of serum albumin. *FASEB J* 1999;**13**:233–44.
23 **Jain A**, Martensson J, Mehta T, *et al*. Ascorbic acid prevents oxidative stress in glutathione-deficient mice: effects on lung type 2 cell lamellar bodies, lung surfactant, and skeletal muscle. *Proc Natl Acad Sci USA* 1992;**89**:5093–7.
24 **Cross CE**, O'Neill CA, Reznick AZ, *et al*. Cigarette smoke oxidation of human plasma constituents. *Ann NY Acad Sci* 1993;**686**:72–89.
25 **Kelly FJ**, Mudway I, Blomberg A, *et al*. Altered lung antioxidant status in patients with mild asthma. *Lancet* 1999;**354**:482–3.
26 **Dauletbaev N**, Viel K, Buhl R, *et al*. Glutathione and glutathione peroxidase in sputum samples of adult patients with cystic fibrosis. *J Cyst Fibros* 2004;**3**:119–24.
27 **Bunnell E**, Pacht ER. Oxidized glutathione is increased in the alveolar fluid of patients with the adult respiratory distress syndrome. *Am Rev Respir Dis* 1993;**148**:1174–8.
28 **Dickinson DA**, Forman HJ. Cellular glutathione and thiols metabolism. *Biochem Pharmacol* 2002;**64**:1019–26.
29 **Holmgren A**. Antioxidant function of thioredoxin and glutaredoxin systems. *Antioxid Redox Signal* 2000;**2**:811–20.
30 **Kinnula VL**. Focus on antioxidant enzymes and antioxidant strategies in smoking related airway diseases. *Thorax* 2005;**60**:693–700.
31 **van der Deen M**, de Vries EG, Timens W, *et al*. ATP-binding cassette (ABC) transporters in normal and pathological lung. *Respir Res* 2005;**6**:59–75.
32 **Paolicchi A**, Lorenzini E, Perego P, *et al*. Extracellular thiol metabolism in clones of human metastatic melanoma with different gamma-glutamyl transpeptidase expression: implications for cell response to platinum-based drugs. *Int J Cancer* 2002;**97**:740–5.
33 **Thomas JA**, Poland B, Honzatko R. Protein sulfhydryls and their role in the antioxidant function of protein S-thiolation. *Arch Biochem Biophys* 1995;**319**:1–9.
34 **Marcy TW**, Merrill WW, Rankin JA, *et al*. Limitations of using urea to quantify epithelial lining fluid recovered by bronchoalveolar lavage. *Am Rev Respir Dis* 1987;**135**:1276–80.
35 **Uejima Y**, Fukuchi Y, Nagase T, *et al*. Influences of inhaled tobacco smoke on the senescence accelerated mouse (SAM). *Eur Respir J* 1990;**3**:1029–36.
36 **Kondo T**, Tagami S, Yoshioka A, *et al*. Current smoking of elderly men reduces antioxidants in alveolar macrophages. *Am J Respir Crit Care Med* 1994;**149**:178–82.
37 **Pratico D**, Basili S, Vieri M, *et al*. Chronic obstructive pulmonary disease is associated with an increase in urinary levels of isoprostane F2alpha-III, an index of oxidant stress. *Am J Respir Crit Care Med* 1998;**158**:1709–14.
38 **Paredi P**, Kharitonov SA, Leak D, *et al*. Exhaled ethane, a marker of lipid peroxidation, is elevated in chronic obstructive pulmonary disease. *Am J Respir Crit Care Med* 2000;**162**:369–73.
39 **Drost EM**, Skwarski KM, Sauleda J, *et al*. Oxidative stress and airway inflammation in severe exacerbations of COPD. *Thorax* 2005;**60**:293–300.

INTERNAL MEDICINE

□ SYMPOSIUM I □

1. COPD Pathogenesis from the Viewpoint of Risk Factors

Shinji Teramoto

Abstract

Chronic obstructive pulmonary disease (COPD) is characterized by irreversible airflow limitation in the lungs. Smoking is one of the amongst major risk factors for the development of COPD. Environmental pollution, age, and airway hyperreactivity are also the risk factors. The protease-antiprotease imbalance and the oxidant-antioxidant imbalance cause airway inflammation and destruction. The genes related to these balances may contribute to development of COPD pathology. Candidate gene-association studies and linkage analyses have been reported for COPD patients. The alpha-1 antitrypsin, glutathione S-transferase, microsomal epoxide hydrolase, and matrix metalloproteinase, are candidate genes. In acquired factors for COPD pathology, the adenoviral latent infection may enhance airway inflammation, leading to airflow obstruction. The current progress and future visions of genetic predisposition of COPD are discussed.

Key words: Smoking, protease-antiprotease imbalance, oxidant-antioxidant imbalance, Gene-Association Studies, adenoviral latent infection may

(DOI: 10.2169/internalmedicine.46.1775)

Introduction

Chronic obstructive pulmonary disease (COPD) is characterized by irreversible airflow limitation in the lungs. Although COPD was the 12th largest disease burden in the world in 1990, it is estimated that it will rise to be the fifth largest disease burden by 2020 (1-4). The most important risk factor for the development of COPD is smoking (Fig. 1). However, only 10-20% of chronic heavy smokers develop symptomatic COPD, which indicates that a difference in susceptibility to tobacco smoke injury must exist and may be related to genetic factors (Fig. 2). Candidate gene-association studies and linkage analyses have been reported for COPD patients. We summarized the evidence for the role of the candidate genes in the pathological processes associated with COPD. This review describes the genetic predisposition of COPD. The current progress and future visions of genetic predisposition of COPD are further addressed.

1) Background and Risk Factors of Development of COOD

Chronic tobacco smoking is the major risk factor for the development of COPD, but only a relatively small proportion of smokers actually develop airway obstruction. Although there is a dose-response relationship between FEV1 and the extent of cigarette smoking, smoking history accounts for only approximately 15% of the variation in lung function. That is why the genetic predisposition of COPD may exist in smokers. Although cigarette smoking is the most important risk factor for the development of COPD, allergic airway inflammation, long-standing asthma, air pollutants, and diesel exhaust particles may also cause irreversible airflow limitation such as COPD. Environmental pollution, age, and airway hyperreactivity are also the risk factors. Destruction of the lung parenchyma leads to the loss of alveolar attachments to the small airways and decreases lung elastic recoil (Fig. 1).

2) Candidate Gene-Association Studies for the Development of COPD

a) The genes related to the protease-antiprotease imbalances

There are two major hypotheses on the cause of COPD and emphysema, such as the protease-antiprotease hypothesis and the oxidant-antioxidant hypothesis (5, 6). It is well known that the Z alpha (1)—antitrypsin homozygote is predisposed to developing early onset basal, panacinar emphy-

Department of Geriatric Medicine, Graduate School of Medicine, The Tokyo University, Tokyo
Correspondence to Dr. Shinji Teramoto, shinjit-tky@umin.ac.jp

DOI: 10.2169/internalmedicine.46.1775

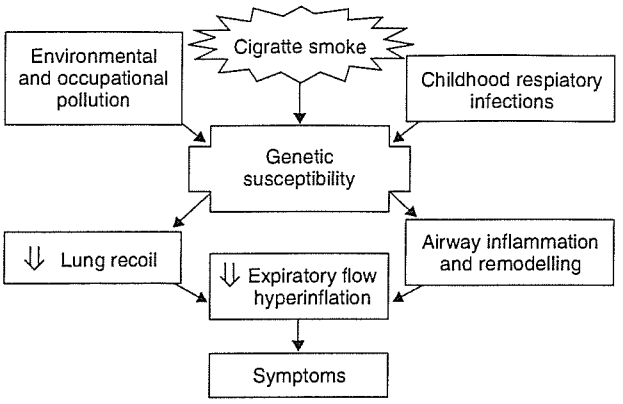

Figure 1. **The risk factors for the development of COPD.**

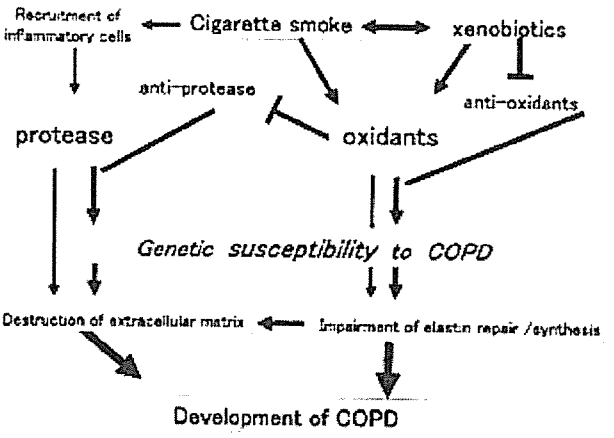

Teramoto S et al. Xenobiotic enzymes and genetics of COPD. Chest 2005 ; 127 : 408-409

Figure 2. **Hypothesis of genetic susceptibility to COPD (6).**

sema (7). In patients with the secretory defect of alpha (1)—antitrypsin, the lung tissue is under uncontrolled proteolytic attack from neutrophil elastase, culminating in alveolar destruction (8-12). The mouse metalloelastase knock-out studies implicate this enzyme as a key mediator in the pathology associated with cigarette smoke-induced emphysema (13, 14). There is also associative evidence from human genetic and animal studies suggesting a pathological link with other MMPs. The polymorphism of alpha-1-antichymotrypsin (AACT) and tissue inhibitor of metalloproteinases-2 (TIMP-2) gene polymorphisms may be associated with individual susceptibility to the development of COPD. The AACT/Ala-15 genotype may be less protective against smoking injury.

b) The genes related to the oxidant-antioxidant imbalance

Oxidative stress is believed to play an important role in the pathogenesis of smoking-induced COPD. The second hypothesis is the oxidant-antioxidant theory, which proposes that oxidant stress and reactive oxygen species (ROS), resulting from an oxidant/antioxidant imbalance, have important consequences for the pathogenesis of COPD. These include oxidative inactivation of antiproteinases, alveolar epithelial injury, increased sequestration of neutrophils in the pulmonary microvasculature, and gene expression of proinflammatory mediators. Several studies have provided supportive evidence of a role for reactive oxygen species (ROS) released from circulating neutrophils and the development of airflow limitation. Thus, the presence of oxidative stress may have important consequences for the pathogenesis of COPD. Number of studies have been done on the identification of genes that predispose to the development of COPD.

Heme oxygenase-1 (HO-1) plays a protective role as an antioxidant in the lung. The length of the (GT)n repeat in the 5'-flanking region of human HO-1 gene polymorphism is associated with susceptibility to COPD (15). The polymorphisms of antioxidant genes glutathione S-transferase M1 (GSTM1) and GSTP1 are reported to be associated with susceptibility to an accelerated decline of lung function in smokers (16, 17).

c) Xenobiotic enzymes and genetics of COPD

Each puff of a cigarette contains 10^{17} free radicals and about 4000 substrates including carcinogenic agents and other possible causative agents of COPD such as volatile aldehydes and hydrogen cyanide. Thus, defects in the detoxification of these reactive species may predispose smokers to airflow obstruction and emphysema. It has been suggested that genetic polymorphisms of cytochrome P450, microsomal epoxide hydrolase (mEPHX) are associated with emphysema or COPD (18-20). The genetic polymorphism of exon 5 of smokers with glutathione S-transferase P1 (GSTP 1) is associated with the development of COPD in smokers (3). There is growing evidence for the role of xenobiotics and antioxidant imbalance in the pathogenesis of airflow obstruction, which is supported by association studies between COPD and variants in epoxide hydrolase and GSTs that detoxify free radicals and other tobacco products (10-14).

d) Other genes associated with the genetic predisposition to COOD

Because airway obstruction is due to both loss of lung elastic recoil and inflammatory narrowing of peripheral airways, genetic polymorphisms that affect either process could be involved. It has been suggested that genetic polymorphisms of tumour necrosis factor-α, interleukin-13 (IL-13) gene promoter, and Vitamin D binding protein gene are associated with emphysema or COPD (21-23).

3) The Pathologic Relationship between Respiratory Illness in Childhood and Chronic Air-Flow Obstruction in Adulthood. —Adenoviral Latent Infection Thytpothesis—

It has been suggested that respiratory illness in childhood might cause chronic air-flow obstruction in adulthood. Hogg